Chapter 2

Structural characterization of glycans on omega-1, a major *Schistosoma mansoni* egg glycoprotein that drives Th2 responses

Moniek HJ Meevissen, Manfred Wuhrer, Michael J Doenhoff, Gabriele Schramm, Helmut Haas, André M Deelder and Cornelis H Hokke

Journal of Proteome Research 2010 9(5):2630-42.

Abstract

Soluble egg antigens (SEA) of the human parasite *Schistosoma mansoni* are among the strongest natural stimuli of Th2 responses. Omega-1, a major glycoprotein in SEA, initiates these characteristic Th2 responses through conditioning of dendritic cells (DCs). In view of the reported immunomodulatory potential of SEA glycans, we have investigated omega-1 glycosylation, using an approach combining mass spectrometric (MS) techniques and enzyme treatments at the glycopeptide level. We demonstrate that omega-1 has two fully occupied N-glycosylation sites, each mainly carrying core-difucosylated diantennary glycans with one or more LeX motifs in the antennae. Using a specific approach of nanoscale LC-MS(/MS) and MALDI-TOF(/TOF)-MS in combination with exo-glycosidase treatments of tryptic glycopeptides, we were able to provide a detailed, site-specific glycosylation analysis of a single, native *S. mansoni* glycoprotein. The obtained knowledge of the glycans present on omega-1 contributes to a full understanding of the mode of action of this immunomodulatory glycoprotein.

Introduction

Schistosomiasis, a disease caused by infection with parasitic flatworms, is a major public health burden in many developing countries in the tropics and sub-tropics. Schistosome larvae released from infested water snails penetrate through the skin of the host, and the developing schistosomes migrate towards the mesenteric venules of the bowel (*Schistosoma mansoni* and *S. japonicum*) or the venous plexus of the bladder (*S. haematobium*), where adult female and male worms pair and produce hundreds of eggs per day. Instead of being excreted with the feces or urine to continue the schistosome life cycle, many of the eggs get trapped inside organs where they induce granulomatous immune reactions, the main cause of morbidity associated with schistosomiasis [1].

During *S. mansoni* infection, an initial T helper 1 (Th1)-mediated response to the parasite shifts to a highly Th2-polarized immune response. This shift coincides with the start of egg production by the mature worms, suggesting that egg-derived molecules are capable of inducing the Th2-polarization [2]. Indeed, schistosome eggs [3], soluble egg antigens (SEA) [4;5], and more specifically a subfraction of SEA formed by the excretory/secretory (ES) egg proteins [6] are highly potent inducers of a Th2 immune response. Recently, the major single factor from ES that is responsible for Th2-priming *in vitro* and *in vivo* has been identified as omega-1, a glycoprotein with RNase activity and a major constituent of ES [7;8]. *In vitro,* omega-1 conditions human monocyte-derived dendritic cells (DCs) to drive Th2-polarization, while SEA depleted from omega-1 shows a significantly reduced activity [6;9]. Furthermore, when injected in IL-4 dual reporter mice, omega-1 is sufficient for Th2-induction *in vivo*. Although is has been suggested that the RNase activity of omega-1 may be involved in its capacity to drive Th2-polarization [9], total SEA requires intact glycosylation to be able to induce Th2-type responses including antigen-specific IgE production and induction of IL-4 and IL-10 [5]. Moreover, synthetic conjugates of the Galβ1-4(Fucα1-3)GlcNAc (Lewis X, LeX) element occurring in SEA have been shown to harbor Th2-promoting properties [10;11]. These observations suggest that glycans or glycan motifs carried by SEA glycoproteins such as omega-1 play a role in the mechanisms by which they exert their Th2-inducing activity.

Schistosome egg glycosylation has been studied extensively, mainly by mass spectrometric analysis of released N- and O-glycans. A wide spectrum of complex and partly stage-specific structures has been found [12-15]. Glycoprotein glycans from SEA comprise high mannose, complex-type and truncated N-glycans which are predominantly α3/α6-difucosylated at the Asn-linked GlcNAc, potentially accompanied by a core-xylose [12]. The non-reducing N-glycan termini are for a large part composed of Galβ1-4GlcNAc (LacNAc, LN), LeX and (mono-

or di-fucosylated) GalNAcβ1-4GlcNAc (LacdiNAc, LDN) motifs [12;13]. Egg glycoprotein O-glycans are mainly based on the mucin-type core 1 (Galβ1-3GalNAc) and core 2 (Galβ1-3(GlcNAcβ1-6)GalNAc) structures, but also a *S. mansoni*-specific Galβ1-3(Galβ1-6)-GalNAc core was found [12,14], while O-glycan termini were mainly composed of LeX, LN and (multi-fucosylated) LDN motifs. Recently, the glycans released from the ES fraction of *S. mansoni* eggs were analyzed, showing that these display N-glycan α3/α6-core fucosylation and terminal LN, LeX and (fucosylated) LDN motifs as main features [15].

Although it is currently debated exactly which proteins make up the ES fraction [16-18] of *S. mansoni* eggs, it is clear that multiple N- and O-glycosylated proteins are present [16]. The presence or absence of specific glycans may confer antigenic properties to individual proteins in ES and influence binding to C-type lectin receptors (CLRs) on immune cells, such as dendritic cell-specific intercellular adhesion molecule-2-grabbing non-integrin (DC-SIGN), mannose receptor (MR) or macrophage galactose-type lectin (MGL) [19-22]. Therefore, it would be appropriate to analyze the glycosylation of ES in a protein-specific fashion, instead of by releasing glycans from the protein mixture and thus losing crucial information about how individual proteins are glycosylated. To date, only in the case of IPSE/α1 [23], another major component of ES, has a protein-specific in-depth glycosylation analysis been carried out [24].

In view of the immunomodulatory properties of omega-1 and the lack of structural information about omega-1 glycans, we performed a detailed analysis of omega-1 glycosylation using nanoscale LC-MS(/MS), and MALDI-TOF(/TOF) MS measurements of tryptic glycopeptides in combination with exo-glycosidase treatments. We show that omega-1 has two fully occupied N-glycosylation sites, which carry mainly core-difucosylated diantennary glycans with one or two terminal LeX motifs. These data provide a molecular basis for investigations on functional properties of omega-1 glycosylation and shed light on the structural details of schistosome egg glycan antigens.

Results

Initial analysis of omega-1 glycosylation

Omega-1 is produced in the subshell area of *S. mansoni* eggs where also IPSE/α1 is produced [8,24]. To investigate whether omega-1, like IPSE/α1, carries LeX motifs [24], purified omega-1 (Figure 1A) was subjected to Western blot analysis. The anti-LeX mAb 128-4F9-A binds to omega-1 (Figure 1B), demonstrating the presence of LeX. Treatment of omega-1 with α-fucosidase to remove terminal α1-3,4-linked fucoses (omega-1 fuco, Figure 1B) strongly reduces binding of the antibody, confirming the presence of the fucosylated LeX motif on omega-1. For subsequent

in depth glycosylation analysis of omega-1, the purified glycoprotein was subjected to SDS-PAGE and the gel piece containing omega-1 was cut, reduced, alkylated and treated with trypsin to generate (glyco)peptides. Extracted (glyco)peptides were subjected to nano-RP-LC-MS analysis. Omega-1 has two concensus glycosylation sites at residues N71 (tryptic peptide Q69-R77) and N176 (tryptic peptide E172-R183) [8]. In the LC chromatogram, based on the observation of the glycosylation marker ions at *m/z* 366 (LN antenna) and *m/z* 512 (LeX antenna), three glycopeptide regions were registered at time windows 7.4-9.3, 14.3-16.9 and 19.3-20.9 minutes (data not shown). The first and second glycopeptide clusters are indistinguishable in terms of glycan heterogeneity and both arise from peptide Q69-R77. Evidently, the glutamine at the amino terminus of the second cluster had undergone cyclization, forming a pyroglutamate, leading to a mass shift of *m/z* - 5.3 $[M+3H]^{3+}$ compared to the glycopeptide cluster with native N-terminal glutamine, and a shift in elution time due to an increase in hydrophobicity upon cyclization. The nano-LC-mass spectrum belonging to the first cluster (site N71) is shown in Figure 2A. The nano-LC-mass spectrum of tryptic glycopeptides containing site N176 which eluted at 19.3-20.9 minutes is shown in Figure 2B.

The glycans of both glycosylation sites are composed of variable numbers of hexoses (H), *N*-acetylhexosamines (N) and fucoses (F), as reflected by corresponding mass differences

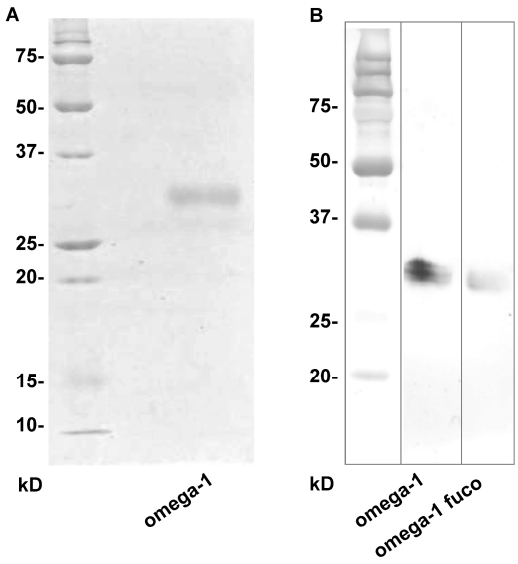

Figure 1. Visualization and characterization of omega-1. Omega-1 was separated under reducing conditions by SDS-PAGE and stained with Colloidal blue (A). For testing the presence of terminal LeX, omega-1 and omega-1 treated with α1-3,4 fucosidase (Omega-1 fuco) were subjected to Western blot using a monoclonal antibody against LeX (128-4F9-A) (B).

(162, 203, and 146 Da, respectively) between the registered glycopeptides. For glycopeptides containing site N71 (Figure 2A), the assumption of a Q69-R77 peptide moiety decorated with an N-glycan leads for the major glycopeptide species ($[M+3H]^{3+}$ at *m/z* 1080.5) to the deduced glycan composition $H_5N_4F_4$. This composition may represent an N-glycan with two LeX antennae and core-difucosylation, which has also been found on IPSE/α1 [15;24]. Other major signals include N-glycans composed of H_5N_4 and H_4N_5 substituted with two to six fucoses, suggesting a high abundance of multi-fucosylated LN and, to a lesser extent, LDN antennae. Tryptic glycopeptides covering site N176 (Figure 2B) were found to contain glycans which were similar in composition to those of site N71. However, ratios of glycan variants were significantly different for the two sites (Figure 2). In general, glycopeptides of site N176 showed a lower degree of fucosylation than those of site N71. Non-glycosylated forms of the peptides Q69-R77 and E172-R183 were not detected by LC-MS, indicating that in both peptides the N-glycosylation sites are fully occupied (data not shown).

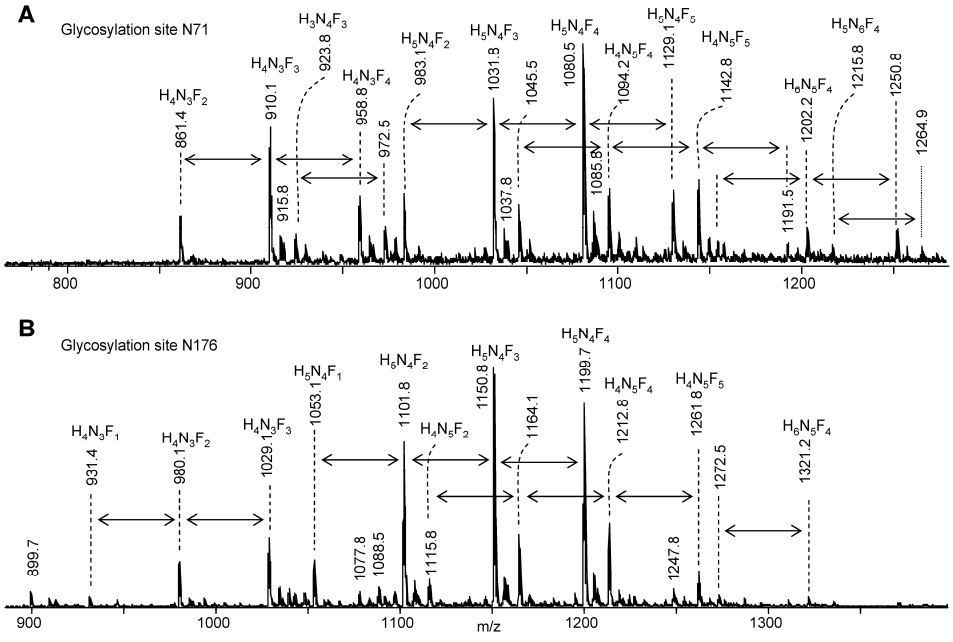

Figure 2. nano-LC-MS of glycopeptides from a tryptic digest of omega-1, covering glycosylation sites N71 (A) and N176 (B). Signals are triple positively charged and labeled with monoisotopic masses. Compositions of the glycan moieties are given in terms of hexose (H), *N*-actetylhexosamine (N) and fucose (F). Differences in fucose content are indicated by double-headed arrows.

N-glycosylation analysis of glycopeptide E172-R183

To confirm the tentative assignment of the glycopeptide clusters presented in Figure 2, the tryptic glycopeptides were subjected to enzymatic treatment with β-galactosidase and/or α-fucosidase and analyzed by MALDI-TOF-MS (Figures 3 and 4). Selected untreated and α-fucosidase treated glycopeptides were in addition subjected to fragmentation using MALDI-TOF/TOF-MS to further substantiate the structural assignments. A set of illustrative glycopeptide fragmentation spectra is shown in Figures 5-7 and Supplementary figures 1 and 2. For the other glycopeptides, the fragmentation data are summarized in Table 1 (untreated) and Supplementary table 1 (α-fucosidase treated). First, we confirmed that the glycopeptides assigned to site N176 (Figure 2B, 3A, and 4A) comprised the peptide moiety E172-R183: for the glycopeptide at *m/z* 3594.7 (Figure 3A), a characteristic MALDI-TOF/TOF-MS pattern of fragment ions was observed (Figure 5), including *m/z* 1370.2 (protonated peptide-NH_3), *m/z* 1470.2 (^{0,2}X-ring fragmentation of the innermost *N*-acetylglucosamine), *m/z* 1736.3 (protonated peptide with *N*-acetylglucosamine and one fucose) and *m/z* 1882.2 (protonated peptide with *N*-acetylglucosamine and two fucoses). This indicates a peptide mass of 1387.3 Da $[M + H]^+$ and a glycan moiety of $H_5N_4F_4$. The deduced peptide mass of 1387.3 Da fits the theoretical mass of the tryptic peptide E172-R183 of 1388.6 Da $[M + H]^+$. In addition, peptide fragments in the low mass region provided a GSANCIR sequence tag that further confirms the assignment. For the other fragmented glycopeptides belonging to the peptide moiety E172-R183 containing glycosylation site N176, similar signal patterns were observed (Figures 6 and 7, Supplementary figures 1 and 2 and Table 1). The combined data from enzymatic treatments and MALDI-TOF/TOF-MS analysis showed that $H_5N_4F_4$ on N176 is an N-glycan constructed of a trimannosyl core with two fucoses on the innermost *N*-acetylglucosamine and two fucosylated LN antennae. Based on the reactivity of omega-1 with an anti-LeX antibody (Figure 1B) and previously published data on the glycosylation of ES proteins including IPSE/α1 [15;24], the fucosylated LN antennae were interpreted as LeX motifs. Both enzyme treatments (Figures 3 and 4) and fragmentation data (Figure 5) are consistent with this interpretation. The galactose β1-4 linkage in a LeX trisaccharide is not cleavable by β-galactosidase because of the 3-substitution of GlcNAc by fucose. In line with the assumption that the $H_5N_4F_4$ species contains two LeX antennae, β-galactosidase treatment did not lead to the disappearance of the signal at *m/z* 3594.7 and at the same time no increased signal at *m/z* 3432.6 was observed (Figures 3A and B). On the other hand, when the glycopeptides were treated with α-fucosidase from *Xanthomonas manihotis*, the fucoses in the LeX motif were removed (loss of signals at *m/z* 3594.7 ($H_5N_4F_4$) and *m/z* 3448.6 ($H_5N_4F_3$); Figure 4A and B), yielding a set of signals at *m/z* 3302.7, 3156.1 and 3010.1 from $H_5N_4F_2$, $H_5N_4F_1$ and H_5N_4 glycoforms, respectively (Figure 4B). Treatment with β-

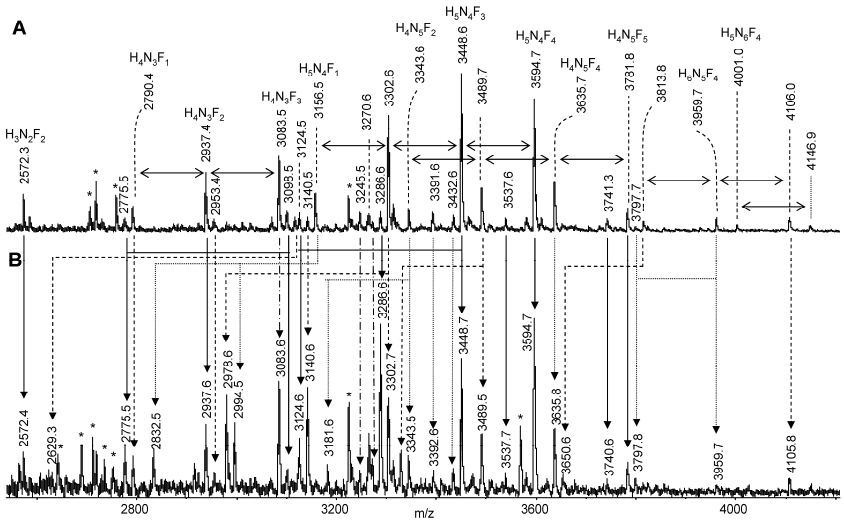

Figure 3. β-galactosidase treatment of omega-1 glycopeptides. Omega-1 was subjected to reduction and alkylation, digested with trypsin and the resulting (glyco)peptides of glycosylation site N176 were analyzed by MALDI-TOF-MS before (A) and after (B) treatment with β-galactosidase. Signals are singly positively charged and labeled with monoisotopic masses. Composition of the glycan moieties are given in terms of hexose (H), *N*-actetylhexosamine (N) and fucose (F). Differences in fucose content are indicated by double-headed arrows. Non-glycopeptide signals are marked with asterisks (*).

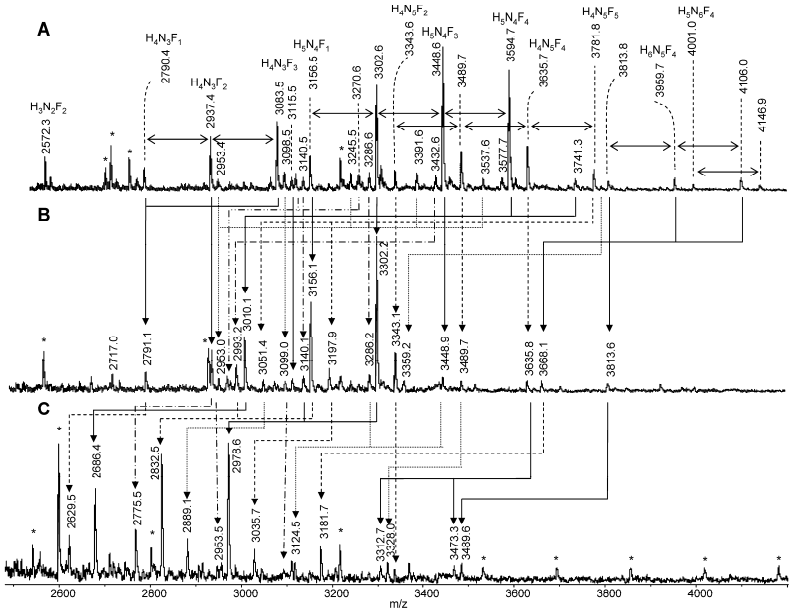

Figure 4. α-fucosidase and β-galactosidase treatment of omega-1 glycopeptides. Omega-1 was subjected to reduction and alkylation, digested with trypsin and the resulting (glyco)peptides of glycosylation site N176 were analyzed by MALDI-TOF-MS before treatment (A), after treatment with α-fucosidase only (B) or in combination with β-galactosidase (C). Signals are singly positively charged and labeled with monoisotopic masses. Composition of the glycan moieties are given in terms of hexose (H), *N*-actetylhexosamine (N) and fucose (F). Differences in fucose content are indicated by double-headed arrows. Non-glycopeptide signals are marked with asterisks (*).

galactosidase subsequent to this fucosidase treatment leads to a complete removal of the antenna galactoses from each of the $H_5N_4F_2$, $H_5N_4F_1$ and H_5N_4 species (shift of two times 162 Da; e.g. the signal at *m/z* 3302.2 in Figure 4B shifts to *m/z* 2978.6 in Figure 4C). The resistance of the $H_5N_4F_4$ glycopeptide to β-galactosidase treatment and the gained susceptibility after α-fucosidase treatment further supports our proposal that the terminal fucosylated structures are LeX motifs. To corroborate this, a MALDI-TOF/TOF-MS fragmentation spectrum of the E172-R183-$H_5N_4F_4$ glycopeptide was recorded (Figure 5) in which the losses of 511 Da and 673 Da (signals at *m/z* 3083.3 and 2920.7) from the parent ion are observed, corresponding to the loss of a LeX ($H_1N_1F_1$) and a LeX-Man fragment ($H_2N_1F_1$), respectively. In addition, a core cleavage pattern with an intense signal at *m/z* 1882.2 (peptide-N_1F_2) (Figure 5) is observed, indicating that two fucose residues in the $H_5N_4F_4$ species are linked to the core GlcNAc residue. The lower intensity signal at *m/z* 1736.3 (peptide-N_1F_1), is interpreted as the result of a chitobiose cleavage in combination with loss of a core fucose. This interpretation was further confirmed by MALDI-TOF/TOF-MS of the E172-R183-$H_5N_4F_2$ glycopeptide species which is formed after the α-fucosidase treatment (Supplementary figure 1). In this spectrum, signals derived from antenna fragmentations are observed at *m/z* 2937.1 and 2774.9 (loss of H_1N_1 and H_2N_1, respectively), but no loss of $H_1N_1F_1$ is observed, indicating that all antenna fucoses had been removed. In addition, the core fragmentation pattern including an intense signal at *m/z* 1882.4 (peptide-N_1F_2) accompanied by a minor signal at *m/z* 1736.4 (loss of one fucose from peptide-N_1F_2), a pattern highly similar to that present in Figure 5, indicates that two core fucoses remain.

A second abundant signal in the MALDI-TOF MS spectrum in Figures 3A and 4A is that of glycopeptide E172-R183-$H_5N_4F_3$. Our data indicate that the $H_5N_4F_3$ species carry two LN antennae and comprise two differentially fucosylated isomers. A fraction of the E172-R183-$H_5N_4F_3$ glycopeptides is resistant to β-galactosidase treatment (part of the signal at *m/z* 3448.6 in Fig. 3A remains in Fig. 3B), which, as previously explained for $H_5N_4F_4$, indicates the presence of two LeX antennae. The other fraction of the glycopeptides exhibited the loss of one hexose after β-galactosidase treatment (loss of 162 Da, resulting in a signal at *m/z* 3286.6 in Figure 3B), which suggests the presence of one non-fucosylated and one fucosylated LN. Based on these results, we suggest that $H_5N_4F_3$ on site N176 consists of two isomeric glycans, one containing two LeX antennae and a mono-fucosylated core, while the other carries one LeX and one LN antenna and two core fucoses. The assumed presence of LeX and LN motifs on the isomers was verified using MALDI-TOF/TOF-MS (Figure 6). The fragmentation spectrum reveals the loss of 511 Da and 673 Da (signals at *m/z* 2937.9 and 2775.5) from the parent ion, corresponding to the loss of a LeX ($H_1N_1F_1$) and a LeX-Man ($H_2N_1F_1$) moiety, respectively. Furthermore, the observed losses of 365 Da and 527 Da (signals at *m/z* 3083.8 and 2921.1) indicate the presence of LN (H_1N_1) and

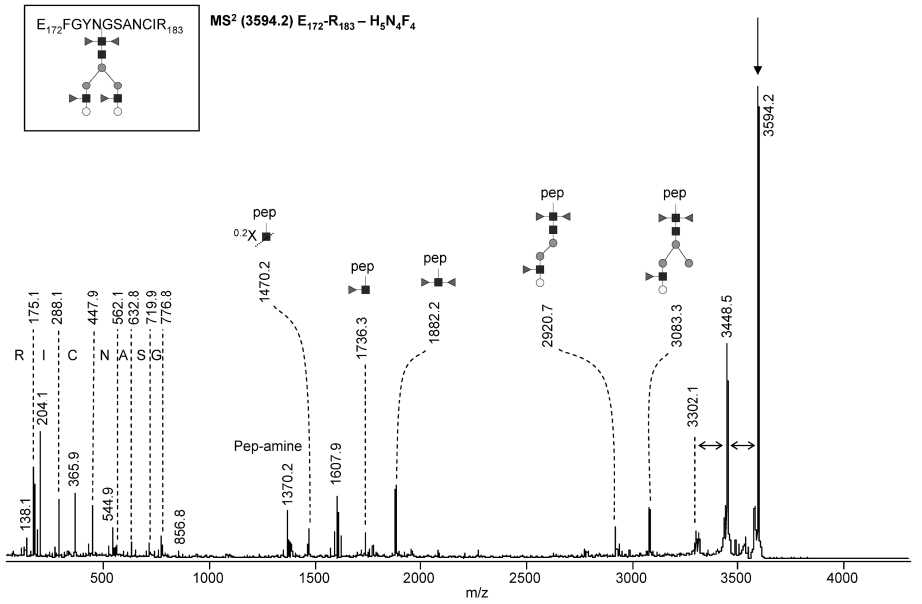

Figure 5. MS/MS of peptide E172–R183 carrying $H_5N_4F_4$ N-glycans. The MS/MS spectrum was acquired by MALDI-TOF/TOF-MS of a tryptic digest of omega-1. The single-headed arrow indicates the precursor ion. Differences in fucose content are indicated by double-headed arrows. Triangle, fucose; light circle, galactose; dark square, *N*-acetylglucosamine; dark circle, mannose.

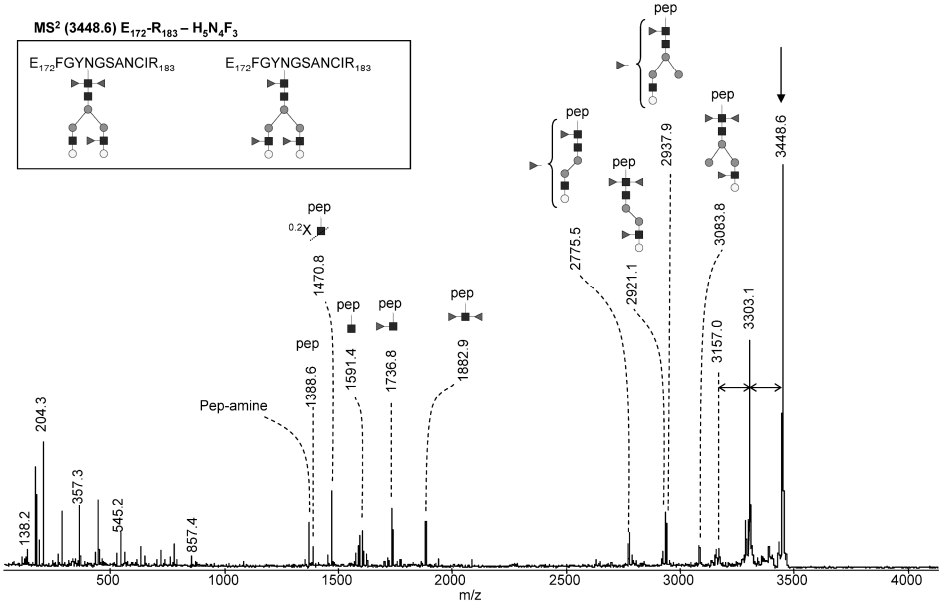

Figure 6. MS/MS of peptide E172–R183 carrying $H_5N_4F_3$ N-glycans. The MS/MS spectrum was acquired by MALDI-TOF/TOF-MS of a tryptic digest of omega-1. The single-headed arrow indicates the parent ion. Differences in fucose content are indicated by double-headed arrows. Triangle, fucose; light circle, galactose; dark square, *N*-acetylglucosamine; dark circle, mannose.

LN-Man (H_2N_1) antennae, respectively, in one of the isomers. In addition, a core cleavage pattern is observed (Figure 6) which clearly differs from the pattern characteristic of core-difucosylation (Figure 5 and Supplementary figure 1). In Figure 6, the signal at *m/z* 1736.8 (pep+N_1F_1) is more intense than the signal at *m/z* 1882.9 (pep+N_1F_2). By comparison with the core cleavage patterns in Figure 5 and Supplementary figure 1, the pattern in Figure 6 can only partially be explained as resulting from an isomer with difucosylated core (left structure in Figure 6). The fragment ion at *m/z* 1736.8 (pep+N_1F_1) is in addition formed by chitobiose cleavage of the second isomer having a monofucosylated core (right structure in Figure 6).

The composition of the $H_4N_5F_4$ variant on glycosylation site N176 indicates the presence of an N-glycan with two fucoses at the Asn-linked GlcNAc, combined with one LeX and one fucosylated LDN antenna, LDN being a common structural element in helminth glycans [28]. The $H_4N_5F_4$ fragmentation data (Supplementary figure 2) are in line with this interpretation. Signals derived from the loss of N_2F_1 (*m/z* 3081.8) and $H_1N_1F_1$ (*m/z* 3124.7) from the precursor ion are observed, as well as the characteristic core fragmentation pattern indicative of a difucosylated core GlcNAc. The mass spectrometric data do not allow differentiation between Fucα1-3GalNAcβ1-4GlcNAc (F-LDN) and GalNAcβ1-4(Fucα1–3)GlcNAc (LDN-F) structures. However, using synthetic F-LDN and LDN-F glycoconjugates [29], the α-fucosidase from *Xanthomonas manihotis* was shown to cleave only the fucose α1-3 linked to the GlcNAc in LDN-F, but not the α1-3 linkage between the fucose and GalNAc in F-LDN (data not shown). α-Fucosidase treatment of omega-1 glycopeptides (Figure 4B) results in removal of antenna fucoses from $H_4N_5F_4$, as the signal at *m/z* 3635.7 in Figure 4A almost completely shifts to signals at *m/z* 3051.4, 3197.1 and 3343.1, representing glycans with one LN and one LDN motif and zero, one or two core fucoses, respectively (Supplementary table 1). Similar shifts were observed for other glycans that carry fucosylated LDN based on their monosaccharide composition (Figure 4B). Therefore, we propose that some glycoforms of omega-1 carry LDN-F motifs, but F-LDN motifs do not occur.

Another representative example of a fragmentation is given by the MALDI-TOF/TOF mass spectrum of E172-R183-$H_6N_5F_5$ which carries one LeX and one dimeric LeX antenna accompanied by two fucoses at the core (Figure 7). The presence of the dimeric LeX motif was demonstrated by a high signal at *m/z* 3082.4 after fragmentation, indicative of the loss of two interlinked LeX elements. The results of the successive treatment of α-fucosidase and β-galactosidase support this interpretation. α-Fucosidase treatment of $H_6N_5F_5$ glycopeptides results in the loss of up to three antenna fucoses (signal at *m/z* 4106.0 in Figure 4A shifts to *m/z* 3813.6 and 3668.1 in Figure 4B). After subsequent treatment with β-galactosidase, the signals at *m/z* 3668.1 and 3813.6 (Figure 4B) shift to *m/z* 3343.1 and 3489.6 respectively (Figure 4C), indicative

Table 1. Omega-1 tryptic glycopeptides

Glycan composition[a]	Glycopeptide signal (*m/z*)[b]	Relative peak height (%)[c]	Fragment ions[d]	Proposed structures[e]
Peptide E_{172}FGY**N**GSANCIR_{18}				
$H_3N_2F_2$	2572.3 (β-gal: 2572.4; -0 Hex) 858.1 $[M+3H]^{3+}$; 1286.6 $[M+2H]^{2+}$	3	1591.4 (pep^1+N_1) 1882.9 ($pep^1+N_1F_2$) FSI-MS/MS: 366.1 (H_1N_1); 528.2 (H_2N_1); 690.3 (H_3N_1)	Trimannosyl core, ^{3,6}F 
$H_3N_3F_2$	2775.5 (β-gal: 2777.5; -0 Hex)	1		HexNAc antenna, ^{3,6}F 
$H_4N_3F_1$	2790.4 (β-gal: 2791.4; -0 Hex, and 2629.3; -1 Hex)	1	1590.6 (pep^1+N_1) 1736.4 ($pep^1+N_1F_1$) 2279.8 ($pep^1+H_3N_2$) -$H_1N_1F_1$	Trimannosyl core, ^{3,6}F 
$H_4N_3F_2$	2937.4 (β-gal: 2937.6; -0 Hex, and 2775.5;-1 Hex); 979.8 $[M+3H]^{3+}$	6	1590.9 (pep^1+N_1) 1737.9 ($pep^1+N_1F_1$; 1.5) 1883.2 ($pep^1+N_1F_2$; 1.0) 2265.0 ($pep^1+H_2N_2F_1$) - $H_2N_1F_1$ 2426.5 ($pep^1+H_3N_2F_1$) - $H_1N_1F_1$ 2572.3 ($pep^1+H_3N_2F_2$) - H_1N_1 ESI-MS/MS: 366.1 (H_1N_1); 512.2 ($H_1N_1F_1$) 868.8 ($pep^1+N_1F_1$; $[M+2H]^{2+}$)	Mixture: 1 Lewis X, monofucosylated core; and: 1 LN, ^{3,6}F 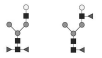 2.5% 3.5%
$H_5N_3F_1$	2953.4 (α-fuc: 2953.0; -0 Fuc)	1		1 LN, mono-fucosylated core 
$H_4N_3F_3$	3083.5 (β-gal: 3083.6; -0 Hex); 1028.5 $[M+3H]^{3+}$	7	1591.4 (pep^1+N_1)1737.2 ($pep^1+N_1F_1$; 0.33)1883.3 ($pep^1+N_1F_2$, 1.0) 2410.8 ($pep^1+H_2N_2F_2$) -$H_2N_1F_1$2426.5 ($pep^1+H_3N_2F_1$) -$H_1N_1F_2$2572.7 ($pep^1+H_3N_2F_2$) -$H_1N_1F_1$ ESI-MS/MS: 366.1 (H_1N_1); 512.2 ($H_1N_1F_1$) 941.9 (pep^1+N1F2; $[M+2H]^{2+}$)	1 Lewis X and ^{3,6}F 
$H_5N_3F_2$	3098.5 (β-gal: 3099.5; -0 Hex, and 2937.6; -1 Hex)	2		Mixture: 1 LN with core and/or antenna fucosylation 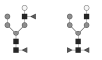 0.5% 1.5%
$H_6N_3F_1$	3115.5 (α-fuc: 3115.1; -0 Fuc)	1		1 LN, mono-fucosylated core
$H_3N_4F_3$	3124.5 (α-fuc: 2978.5; -1 Fuc)	2		1 fucosylated LDN, ^{3,6}F
$H_4N_4F_2$	3140.5 (α-fuc: 3140.1; -0 Fuc)	1		1 LN and 1 HexNAc, ^{3,6}F 
$H_5N_4F_1$	3156.5 (β-gal: 2994.5; -1 Hex, and 2832.5; -2 Hex); 1052.8 $[M+3H]^{3+}$	4	1591.4 (pep^1+N_1) 1737.2 ($pep^1+N_1F_1$) 2483.8 ($pep^1+H_3N_3$) -$H_2N_1F_1$ 2629.1 ($pep^1+H_3N_3F_1$) -H_2N_1 2646.4 ($pep^1+H_4N_3$) -$H_1N_1F_1$ 2792.0 ($pep^1+H_4N_3F_1$) -H_1N_1 ESI-MS/MS: 366.1 (H_1N_1); 512.2 ($H_1N_1F_1$) 868.8 ($pep^1+N_1F_1$; $[M+2H]^{2+}$)	Mixture: biantennary LN with one fucoses at the core or antenna 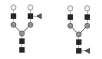 2.5% 1.5%
$H_5N_3F_3$	3245.5 (β-gal: 3245.5; -0 Hex)	2	1881.3 ($pep^1+N_1F_2$)	1 Lewis X, ^{3,6}F 
$H_3N_4F_4$	3270.6 (β-gal: 3270.5; -0 Hex; α-fuc: 2978.5)	1		^{3,6}F
$H_4N_4F_3$	3286.6 (β-gal: 3286.6; -0 Hex, and 3124.6; -1 Hex)	2	1592.0 (pep^1+N_1) 1737.0 ($pep^1+N_1F_1$; 1.0) 1883.3 ($pep^1+N_1F_2$; 1.0) 2630.2 ($pep^1+H_3N_3F_1$) -$H_1N_1F_2$ 2773.7 ($pep^1+H_3N_3F_2$) -$H_1N_1F_1$ 2919.9 ($pep^1+H_3N_3F_3$) -H_1N_1	1 Lewis X or fucosylated GlcNAc, ^{3,6}F  1.0% 1.0%

Table 1. Omega-1 tryptic glycopeptides, continued

Glycan composition[a]	Glycopeptide signal (*m/z*)[b]	Relative peak height (%)[c]	Fragment ions[d]	Proposed structures[e]
Peptide E_{172}FGY**N**GSANCIR_{18}				
$H_5N_4F_2$	3302.6 (β-gal: 3302.7; -0 Hex, 3140.6: -1 Hex, and 2978.6: -2 Hex); 1101.5 $[M+3H]^{3+}$	12	1592.0 (pep^1+N_1) 1737.0 ($pep^1+N_1F_1$; 1.0) 1883.3 ($pep^1+N_1F_2$; 1.0) 2630.2 ($pep^1+H_3N_3F_1$) -$H_1N_1F_2$ 2773.7 ($pep^1+H_3N_3F_2$) -$H_1N_1F_1$ 2919.9 ($pep^1+H_3N_3F_3$) -H_1N_1	Mixture: biantennary LN with core and/or antenna fucosylation 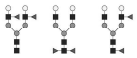 4.5% 4.0% 3.5%
$H_4N_5F_2$	3343.6 (β-gal: 3343.5; -0 Hex, and 3181.6; -1 Hex)	2	1590.3 (pep^1+N_1) 1736.3 ($pep^1+N_1F_1$; 1.0) 1882.4 ($pep^1+N_1F_2$; 1.0) 2628.7 ($pep^1+H_3N_3F_1$) -$H_2N_1F_1$ 2775.1 ($pep^1+H_3N_3F_2$) -H_2N_1 2789.7 ($pep^1+H_4N_3F_1$) -$H_1N_1F_1$ 2937.1 ($pep^1+H_4N_3F_2$) -H_1N_1 ESI-MS/MS: 366.1 (H_1N_1); 512.2 ($H_1N_1F_1$) 941.9 ($pep^1+N_1F_2$; $[M+2H]^{2+}$)	Mixture: biantennary (1 LN, 1 LDN) with core and/or antenna fucosylation 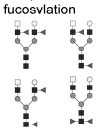 1.0% 1.0%
$H_5N_3F_4$	3391.6 (β-gal: 3391.6; -0 Hex)	2	1591.3 (pep^1+N_1) 2880.4 ($pep^1+H_4N_3F_3$) -$H_1N_1F_1$ 3080.4 ($pep^1+H_4N_3F_3$) -H_1F_1	1 Lewis X and 1 fucosylated mannose, ^{3,6}F 
$H_4N_4F_4$	3432.6 (β-gal: 3432.6; -0 Hex)	1		1 Lewis X and 1 fucosylated HexNAc, ^{3,6}F 
$H_5N_4F_3$	3448.6 (β-gal: 3448.7; -0 Hex, 3286.6; -1 Hex); 1150.2 $[M+3H]^{3+}$	16	1591.4 (pep^1+N_1) 1736.8 ($pep^1+N_1F_1$; 1.3) 1883.0 ($pep^1+N_1F_2$; 1.0) 2629.4 ($pep^1+H_3N_3F_1$) -$H_2N_1F_2$ 2775.5 ($pep^1+H_3N_3F_2$) -$H_2N_1F_1$ 2789.9 ($pep^1+H_4N_3F_1$) -$H_1N_1F_2$ 2921.1 ($pep^1+H_3N_3F_3$) -H_2N_1 2937.8 ($pep^1+H_4N_3F_2$) -$H_1N_1F_1$ 3083.8 ($pep^1+H_4N_3F_3$) -H_1N_1 ESI MS/MS: 366.1 (H_1N_1); 512.2 ($H_1N_1F_1$) 942.0 ($pep^1+N_1F_2$; $[M+2H]^{2+}$)	Mixture: biantennary LN with core and antenna fucosylation  8.0% 8.0%
$H_4N_5F_3$	3489.7 (β-gal: 3489.5; -0 Hex, and 3327.7; -1 Hex); 1163.8 $[M+3H]^{3+}$	4	1591.5 (pep^1+N_1) 1736.7 ($pep^1+N_1F_1$; 0.33) 1883.3 ($pep^1+N_1F_2$; 1.0) 2774.8 ($pep^1+H_3N_3F_2$) -$H_1N_2F_1$ 2816.9 ($pep^1+H_2N_4F_2$) -$H_2N_1F_1$ 2937.0 ($pep^1+H_4N_3F_2$) -N_2F_1 2976.9 ($pep^1+H_3N_4F_2$) -$H_1N_1F_1$ 3080.4 ($pep^1+H_4N_3F_3$) -N_2 3124.1 ($pep^1+H_3N_4F_3$) -H_1N_1 ESI-MS/MS: 366.1 (H_1N_1); 512.2 ($H_1N_1F_1$); 553.3 (N_2F_1)	Mixture: biantennary (1 LN, l LDN) with one antenna fucose, ^{3,6}F  1.5% 2.5%
$H_5N_3F_5$	3537.6 (β-gal: 3537.7; -0 Hex)	1		Lewis X, ^{3,6}F
$H_5N_4F_4$	3594.7 (β-gal: 3594.7; -0 Hex); 1198.9 $[M+3H]^{3+}$	14	1590.9 (pep^1+N_1) 1736.3 ($pep^1+N_1F_1$; 0.33) 1882.2 ($pep^1+N_1F_2$; 1.0) 2774.2 ($pep^1+H_3N_3F_2$) -$H_2N_1F_2$ 2920.7 ($pep^1+H_3N_3F_3$) -$H_2N_1F_1$ 2936.5 ($pep^1+H_4N_3F_2$) -$H_1N_1F_2$ 3083.3 ($pep^1+H_4N_3F_3$) - H_1N_1F,ESI-MS/MS: 366.1 (H_1N_1); 512.2 ($H_1N_1F_1$) 942.0 ($pep^1+N_1F_2$; $[M+2H]^{2+}$)	2 Lewis X, ^{3,6}F 
$H_4N_5F_4$	3635.7 (β-gal: 3635.8; -0 Hex); 1212.5 $[M+3H]^{3+}$	5	1590.4 (pep^1+N_1) 1736.3 ($pep^1+N_1F_1$; 0.33) 1882.3 ($pep^1+N_1F_2$; 1.0) 2774.3 ($pep^1+H_3N_3F_2$) -$H_1N_2F_2$ 2920.8 ($pep^1+H_3N_3F_3$) -$H_1N_2F_1$ 2936.5 ($pep^1+H_4N_3F_2$) -N_2F_2 3081.8 ($pep^1+H_4N_3F_3$) -N_2F_1 3124.7 ($pep^1+H_3N_4F_3$) -$H_1N_1F_1$ ESI-MS/MS: 366.1 (H_1N_1); 512.2 ($H_1N_1F_1$); 553.2 (N_2F_1)	1 Lewis X, 1 fucosylated LDN and ^{3,6}F 

Table 1. Omega-1 tryptic glycopeptides, continued

Glycan composition[a]	Glycopeptide signal (*m/z*)[b]	Relative peak height (%)[c]	Fragment ions[d]	Proposed structures[e]
Peptide E_{172}FGY**N**GSANCIR$_{18}$				
$H_5N_4F_5$	3741.0 (β-gal: 3740.6; -0 Hex)	1	1590.8 (pep^1+N_1) 1737.5 (pep^1+N_1F_1; 0.12) 1883.4 (pep^1+N_1F_2; 1.0) 2937.5 (pep^1+$H_4N_3F_2$) -$H_1N_1F_3$ 3082.4 (pep^1+$H_4N_3F_3$) -$H_1N_1F_2$	1 Lewis X and 1 pseudo LewisY, ^{3,6}F 
$H_4N_5F_5$	3781.8 (β-gal: 3781.6; -0 Hex)	2	1591.1 (pep^1+N_1) 1737.5 (pep^1+N_1F_1; 0.2) 1882.9 (pep^1+N_1F_2; 1.0) 2923.1 (pep^1+$H_3N_3F_3$) -$H_1N_2F_2$ 3083.8 (pep^1+$H_4N_3F_3$) -N_2F_2 3109.1 (pep^1+$H_2N_4F_4$) -$H_2N_1F_1$	1 Lewis X and 1 difucosylated LDN, ^{3,6}F 
$H_5N_5F_4$	3797.7 (β-gal: 3979.8; -0 Hex; α-fuc: 3359.2; -2 Fuc)	1		^{3,6}F
$H_6N_5F_3$	3813.8 (β-gal: 3650.6; -1 Hex)	1		Mixture: biantennary (1 LN, 1 di LN) with core and antenna fucosylation  One of several possible isomers is shown
$H_6N_5F_4$	3959.7 (β-gal: 3959.7; -0 Hex, and 3797.7; -1 Hex)	1	1592.4 (pep^1+N_1) 1737.5 (pep^1+N_1F_1; 0.33) 1883.8 (pep^1+N_1F_2; 1.0) 2776.4 (pep^1+$H_3N_3F_2$) -$H_3N_2F_2$ 2940.2 (pep^1+$H_4N_3F_2$) -$H_2N_2F_2$ 3085.2 (pep^1+$H_4N_3F_3$) -$H_2N_2F_1$ 3302.1 (pep^1+$H_5N_4F_2$) -$H_1N_1F_2$ 3450.7 (pep^1+$H_5N_4F_3$) -$H_1N_1F_1$ 3596.0 (pep^1+$H_5N_4F_4$) -H_1N_1	Mixture: biantennary (1 LN, 1 di-LN) with core and antenna fucosylation  One of several possible isomers is shown.
$H_5N_6F_4$	4001.0	1	1592.7 (pep^1+N_1) 1737.5 (pep^1+N_1F_1; 0.25) 1884.7 (pep^1+N_1F_2; 1.0) 2939.9 (pep^1+$H_4N_3F_2$) -$H_1N_3F_2$ 3302.5 (pep^1+$H_5N_4F_2$) -N_2F_2 3448.9 (pep^1+$H_5N_4F_3$) -N_2F_1 3593.3 (pep^1+$H_5N_4F_4$) -N_2	Mixture: 1 LN and LN-LDN or 1 LDN and di-LN, with core and antenna fucosylation  One of several possible isomers is shown
$H_6N_6F_5$	4106.0 [(β-gal: 4105.8; -0 Hex)	1	1590.4 (pep^1+N_1) 1882.3 (pep^1+N_1F_2;) 2920.5 (pep^1+$H_3N_3F_3$) -$H_3N_2F_2$ 3082.4 (pep^1+$H_4N_3F_3$) -$H_2N_2F_2$ 3299.3 (pep^1+$H_5N_4F_2$) -$H_1N_1F_3$ 3447.5 (pep^1+$H_5N_4F_3$) -$H_1N_1F_2$ 3596.3 (pep^1+$H_5N_4F_4$) -$H_1N_1F_1$	1 Lewis X, 1 di-Lewis X, ^{3,6}F 
$H_5N_6F_5$	4146.9	1	1591.4 (pep^1+N_1) 1737.5 (pep^1+N_1F_1; 0.1) 1883.3 (pep^1+N_1F_2; 1.0) 3083.8 (pep^1+$H_4N_3F_3$) -$H_1N_3F_2$ 3303.6 (pep^1+$H_5N_4F_2$) -N_2F_3 3447.8 (pep^1+$H_5N_4F_3$) -N_2F_2 3594.7 (pep^1+$H_5N_4F_4$) -N_2F_1	Mixture: 1 LN and LN-LDN or 1 LDN and di-LN, with core and antenna fucosylation  One of several possible isomers is shown
Peptide Q_{69}P**N**CTGSLR$_{77}$				
$H_4N_3F_2$	861.4 $[M+3H]^{3+}$ (β-gal: 861.4; -0 Hex, 807.7; -1 Hex)	4	ESI-MS/MS: 366.1 (H_1N_1); 512.2 ($H_1N_1F_1$); 528.2 (H_2N_1) 618.2 (pep^2+N_1; $M+2H]^{2+}$); 691.4 (pep^2+N_1F_1; $[M+2H]^{2+}$); 764.4 (pep^2+N_1F_2; $[M+2H]^{2+}$)	Mixture: 1 LN with core and/or antenna fucosylation  3.0% 1.0%
$H_4N_3F_3$	910.1 $[M+3H]^{3+}$ (β-gal: 910.1; -0 Hex)	10	ESI-MS/MS: 366.1 (H_1N_1); 512.2 ($H_1N_1F_1$) 691.4 pep^2+N_1F_1; $[M+2H]^{2+}$) 764.4 (pep^2+N_1F_2; $[M+2H]^{2+}$)	1 Lewis X, ^{3,6}F 
$H_5N_3F_2$	915.8 $[M+3H]^{3+}$ (β-gal. 915.8, -0 Hex, 807.7; -1 Hex)	2		Mixture: 1 LN with core and/or antenna fucosylation 

Table 1. Omega-1 tryptic glycopeptides, continued

Glycan composition[a]	Glycopeptide signal (*m/z*)[b]	Relative peak height (%)[c]	Fragment ions[d]	Proposed structures[e]
Peptide Q_{69}PNCTGSLR$_{77}$				
$H_3N_4F_3$	923.7 $[M+3H]^{3+}$ (β-gal: 923.7; -0 Hex)	2		
$H_4N_4F_2$	929.8 $[M+3H]^{3+}$	1		
$H_4N_5F_4$	958.8 $[M+3H]^{3+}$ (β-gal: 958.8; -0 Hex)	5	ESI-MS/MS: 366.1 (H_1N_1); 512.2 ($H_1N_1F_1$)691.4 pep^2+N_1F_1; $[M+2H]^{2+}$)764.4 (pep^2+N_1F_2; $[M+2H]^{2+}$)	Lewis X, ^{3,6}F
$H_5N_3F_3$	964.4 $[M+3H]^{3+}$ (β-gal: 964.4; -0 Hex)	2		1 Lewis X, ^{3,6}F 
$H_3N_4F_4$	972.5 $[M+3H]^{3+}$ (β-gal: 972.5; -0 Hex)	3		^{3,6}F
$H_4N_4F_3$	977.8 $[M+3H]^{3+}$ (β-gal: 977.8; -0 Hex)	1		1 Lewis X and 1 HexNAc, ^{3,6}F 
$H_5N_4F_2$	983.1 $[M+3H]^{3+}$ (β-gal: 983.1; -0 Hex, 929.8; -1 Hex, 875.1; -2 Hex)	5	ESI-MS/MS: 366.1 (H_1N_1); 512.2 ($H_1N_1F_1$)691.4 pep^2+N_1F_1; $[M+2H]^{2+}$)764.4 (pep^2+N_1F_2; $[M+2H]^{2+}$)	Mixture: biantennary LN with core and/or antenna fucosylation 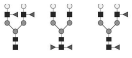 1.0% 2.0% 2.0%
$H_3N_5F_3$	991.4 $[M+3H]^{3+}$ (β-gal: 991.5; -0 Hex)	1		
$H_5N_4F_3$	1031.8 $[M+3H]^{3+}$ (β-gal: 1031.8; 0 Hex, 977.8; 1 Hex)	12	ESI-MS/MS: 366.1 (H_1N_1); 512.2 ($H_1N_1F_1$)764.4 (pep^2+N_1F_2; $[M+2H]^{2+}$)	Mixture: biantennary LN with core and antenna fucosylation  8.0% 4.0%
$H_4N_5F_3$	1045.5 $[M+3H]^{3+}$ (β-gal: 1045.5; -0 Hex, 991.5; -1 Hex)	5	ESI-MS/MS: 366.1 (H_1N_1); 407.2 (N_2); 512.2 ($H_1N_1F_1$); 553.2 (N_2F_1)764.4 (pep^2+N_1F_2; $[M+2H]^{2+}$)	Mixture: Lewis X or fucosylated LDN. ^{3,6}F  2.0% 3.0%
$H_5N_4F_4$	1080.5 $[M+3H]^{3+}$ (β-gal: 1080.5; -0 Hex, 1026.4; -1 Hex)	16	ESI-MS/MS: 366.1 (H_1N_1); 512.2 ($H_1N_1F_1$); 658.2 ($H_1N_1F_2$); 691.4 (pep^2+N_1F_1; $[M+2H]^{2+}$); 764.4 (pep^2+N_1F_2; $[M+2H]^{2+}$)	Mixture: 2 Lewis X, ^{3,6}F or 1 LN with two fucoses, ^{3,6}F  14.0% 2.0%
$H_6N_4F_3$	1086.2 $[M+3H]^{3+}$ (β-gal: 1086.2; -0 Hex)	4	ESI-MS/MS. 366.1 (H_1N_1); 512.2 ($H_1N_1F_1$)	Lewis X, ^{3,6}F
$H_4N_5F_4$	1094.2 $[M+3H]^{3+}$ (β-gal: 1094.1; -0 Hex)	5	ESI-MS/MS: 366.1 (H_1N_1); 407.2 (N_2); 512.2 ($H_1N_1F_1$); 553.2 (N_2F_1)	1 Lewis X, 1 fucosylated LDN and ^{3,6}F 
$H_5N_5F_3$	1099.8 $[M+3H]^{3+}$ (β-gal: 1099.8; -0 Hex)	2		
$H_5N_4F_5$	1129.1 $[M+3H]^{3+}$ (β-gal: 1129.1; -0 Hex)	5	ESI-MS/MS: 366.1 (H_1N_1); 512.2 ($H_1N_1F_1$); 658.2 ($H_1N_1F_2$); 764.4 (pep^2+N_1F_2; $[M+2H]^{2+}$)	1 Lewis X and 1 difucosylated LN, ^{3,6}F 
$H_4N_5F_5$	1142.8 $[M+3H]^{3+}$ (β-gal: 1142.8; -0 Hex)	6	ESI-MS/MS: 366.1 (H_1N_1); 407.2 (N_2); 512.2 ($H_1N_1F_1$); 553.2 (N_2F_1); 658.2 (H1N1F2); 699.2 (N2F2) 764.4 (pep^2+N1F2; $[M+2H]^{2+}$)	Mixture: 1 LN and 1 LDN with 3 antenna fucoses, ^{3,6}F  3.0% 3.0%
$H_5N_5F_4$	1148.5 $[M+3H]^{3+}$ (β-gal: 1148.2; -0 Hex)	1		
$H_6N_5F_3$	1153.5 $[M+3H]^{3+}$ (β-gal: 1099.8; -1 Hex)	1		Mixture: biantennary (1 LN, 1 di-LN) with core and antenna fucosylation

Table 1. Omega-1 tryptic glycopeptides, continued

Glycan composition[a]	Glycopeptide signal (*m/z*)[b]	Relative peak height (%)[c]	Fragment ions[d]	Proposed structures[e]
Peptide Q_{69}**PN**CTGSLR_{77}				
$H_4N_5F_6$	1191.5 $[M+3H]^3$	1		
$H_6N_5F_4$	1202.2 $[M+3H]^{3+}$ (β-gal: 1202.5; -0 Hex, 1148.2; -1 Hex)	2		Mixture: biantennary (1 LN, 1 di-LN) with core and antenna fucosylation
$H_5N_6F_4$	1215.8 $[M+3H]^{3+}$	1		Mixture: 1 LN and LN-LDN or 1 LDN and di-LN, with core and antenna fucosylation
$H_6N_5F_5$	1250.8 $[M+3H]^{3+}$ (β-gal: 1250.8; -0 Hex)	2		Mixture: 1 LN, 1 di-LN with core and antenna fucosylation
$H_5N_6F_5$	1264.9 $[M+3H]^{3+}$	1		Mixture: 1 LN and LN-LDN or 1 LDN and di-LN, with core and antenna fucosylation

a Glycan compositions are given in terms of hexose (H), *N*-acetylhexosamine (N) and fucose (F).
b Monoisotopic masses of glycopeptide precursors are given throughout. Glycopeptides are singly positively charged, unless specified otherwise. Singly-charged glycopeptide species were registered by MALDI-TOF-MS, and multiply charged species were detected by LC-ESI-MS. For many glycopeptides, masses after β-galactosidase (β-gal) and/or α-fucosidase (α-fuc) treatment are listed and the loss of n hexose or n fucose is concluded (respectively - n Hex and - n Fuc).
c Relative peak height is expressed as a percentage of cumulative peak height per site.
d Fragment ions were determined by MALDI-TOF/TOF-MS unless specified otherwise (ESI-MS/MS indicates analysis by nano-HPLC ESI-ion trap-MS/MS); pep1 corresponds to peptide E172FGYNGSANCIR183 containing glycosylation site N176; pep2 corresponds to peptide Q69PNCTGSLR77 containing glycosylation site N71.
e Proposed glycan structures are deduced from glycopeptide MS after enzyme treatments and fragmentation data. Triangle, fucose; light circle, galactose; light square, *N*-acetylgalactosamine; dark square, *N*-acetylglucosamine; dark circle, mannose. Glycan isomer percentages are calculated using the relative peak heights of glycopeptides after β-galactosidase treatment and/or relative peak heights of peptides after fragmentation.

of the loss of two galactoses. This observation is in line with the occurrence of one non-susceptible internal galactose in the proposed structure of $H_6N_5F_5$. In addition to the aforementioned signals, a signal at *m/z* 3181.7 appears, which might be interpreted as the loss of three galactoses from the signal at *m/z* 3668.1. However, we believe that the latter signal is not derived from fucosidase/galactosidase treatment of $H_6N_5F_5$, but arises from $H_4N_5F_2$ (*m/z* 3343.1 in Figure 4B), which represents a core difucosylated glycopeptide with one LN and one LDN antenna. Upon β-galactosidase treatment, the $H_4N_5F_2$ glycoform loses one galactose residue from the LN antenna, thereby giving rise to a signal at *m/z* 3181.7 in Figure 4C, derived from the similar intense signal at *m/z* 3343.1 in Figure 4B.

In a similar manner, combination of fragmentation analysis by MALDI-TOF/TOF-MS and α-fucosidase/β-galactosidase treatment led to structure proposals for most other glycoforms observed for the E172-R183 peptide. The data are summarized in Table 1 and Supplementary table 1.

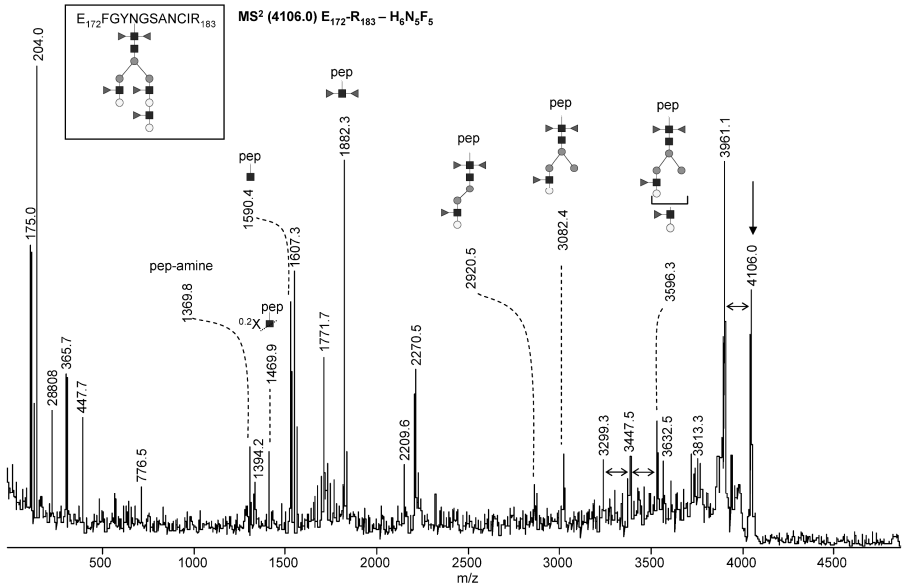

Figure 7. MS/MS of peptide E172–R183 carrying $H_6N_5F_5$ N-glycans. The MS/MS spectrum was acquired by MALDI-TOF/TOF-MS of a tryptic digest of omega-1. The single-headed arrow indicates the parent ion. Differences in fucose content are indicated by double-headed arrows. Triangle, fucose; light circle, galactose; dark square, *N*-acetylglucosamine; dark circle, mannose.

N-glycosylation analysis of glycopeptide Q69-R77

Unlike from the E172-R183 glycopeptides, signals from peptide Q69-R77 containing the glycosylation site N71 could not be detected by MALDI-TOF-MS. The most abundant Q69-R77 glycopeptide, carrying a $H_5N_4F_4$ glycan (Figure 2A), would correspond to a $[M+H]^+$ ion of a theoretical mass of 3095.4 Da, but this was not observed in the spectrum in Figure 3A, nor were any other signals detected that would correspond to glycopeptides from Q69-R77. Therefore, with the specific aim of further characterizing the glycosylation of the Q69-R77 glycopeptides, untreated and β-galactosidase-treated glycopeptides from omega-1 were also measured by nano-LC-MS (Figure 8) and LC-MS/MS (Figure 9 and Table 1). Registered masses, fragmentation data as well as deduced glycan compositions for all the detected glycopeptide species are given in Table 1.

For the most abundant glycopeptide of Q69-R77 carrying the N-glycan $H_5N_4F_4$, the main structure is composed of a trimannosyl core with two fucoses attached to the innermost *N*-acetylglucosamine and two LeX antennae (left structure in Figure 9), using similar reasoning as for the $H_5N_4F_4$ glycan on site N176. However, ~15% of the $H_5N_4F_4$ glycans on site N71 contain a non-fucosylated LN antenna, as demonstrated by the removal of one hexose after β-

galactosidase treatment (*m/z* 1080.5 $[M+H]^{3+}$ in Figure 8A shifts to *m/z* 1026.4 in Figure 8B). This indicates that two fucoses are located at the other LN branch. To verify this, the $H_5N_4F_4$ glycopeptide was fragmented using nano-LC-MS/MS (Figure 9). Losses of 365 Da and 657 Da (signals at *m/z* 1437.6 and 1291.6) were observed from the parent ion, which corresponds to the loss of LN (H_1N_1) and difucosylated LN ($H_1N_1F_2$), respectively. Notably, fragmentation data of protonated glycans and glycopeptides may be compromised due to the occurrence of fucose rearrangements, possibly contributing to the generation of the above described fragments. This phenomenon is commonly seen in the analysis of N-glycans by MALDI as LC-MS fragmentation [30]. However, based on the results from the β-galactosidase treatment, it was clearly demonstrated that a small part of $H_5N_4F_4$ glycans on site N71 contain one LN and one difucosylated LN antenna, a glycan structure which was not observed for $H_5N_4F_4$ on site N176. In analogy with this, we propose for glycopeptide Q69-R77 containing an N-glycan with composition $H_4N_5F_5$ a similar structural assignment as for $H_4N_5F_4$, being one isomer with a difucosylated core in combination with one mono-fucosylated LDN and one difucosylated LN antenna, and another with a difucosylated core and one LeX and one difucosylated LDN antenna (Table 1).

For most of the other N-glycans at site N71, similar information was obtained, as summarized in Table 1. Most of the glycan structures at site N71 were identical to the structures of glycosylation site N176, however in some cases with differences in fucosylation as described above. The main differences between the sites are in the relative abundance of glycan structures, with site N71 containing a higher amount of multi-fucosylated structures compared to site N176.

General overview of omega-1 glycosylation

An overview of the most abundant glycosylation forms of omega-1, combining the data from glycosylation sites N71 and N176, is given in Table 2. Notably, the abundance of individual glycan structures was calculated using signal intensities derived from LC-MS data for site N71 (Figure 10A) and MALDI-TOF-MS data for site N176 (Figure 3A), which might have implications for the comparability of the two sites. On the other hand, when comparing the LC-MS derived data (Figure 2A) and MALDI derived data (Figure 3A) from site N176, the ratio of the high intensity signals are very comparable, although the low abundant species show some deviations.

The majority of the glycan structures on the two sites exhibit two fucoses on the innermost *N*-acetylglucosamine and one or two LeX antennae. In view of the documented immunogenic properties of LeX and core fucosylation [10;31], we estimated the abundance of these structures on omega-1 using the most abundant glycans as markers (Table 2).

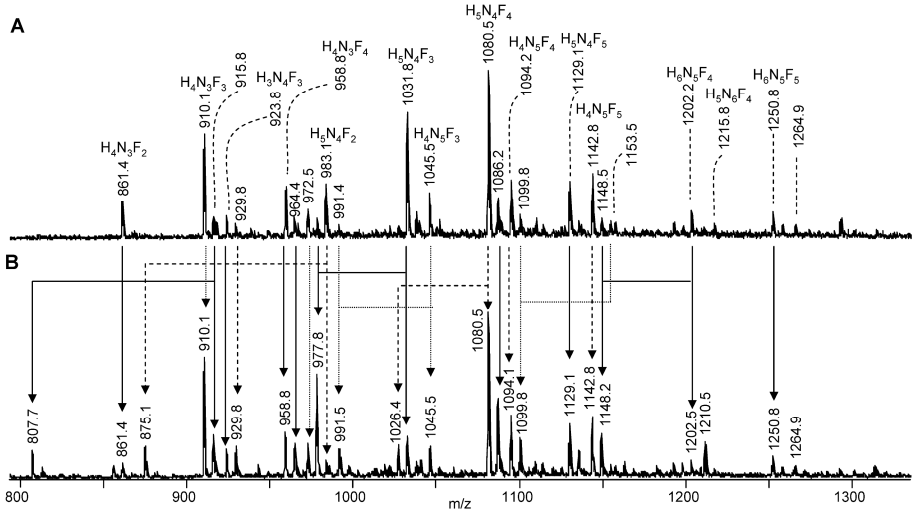

Figure 8. β-galactosidase treatment of omega-1 glycopeptides. Omega-1 was subjected to reduction and alkylation, digested with trypsin and the resulting (glyco)peptides of glycosylation site N71 were analyzed by nano-LC-MS before (A) and after (B) treatment with β-galactosidase. Signals are triple positively charged and labeled with monoisotopic masses. Composition of the glycan moieties are given in terms of hexose (H), N-acetylhexosamine (N) and fucose (F).

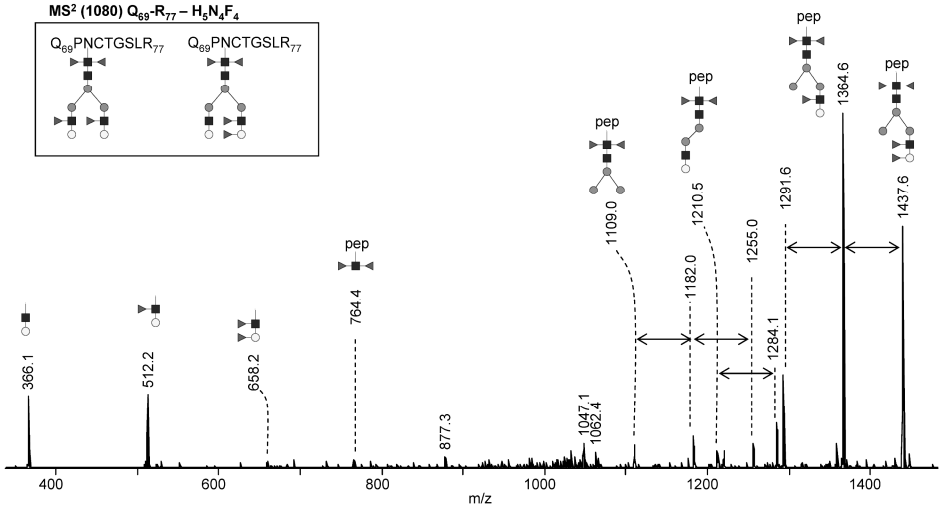

Figure 9. MS/MS of peptide Q69–R77 carrying $H_5N_4F_4$ N-glycans. The MS/MS spectrum was acquired by nano-LC-MS/MS of a tryptic digest of omega-1. Differences in fucose content are indicated by double-headed arrows. Triangle, fucose; light circle, galactose; dark square, *N*-acetylglucosamine; dark circle, mannose.

One omega-1 glycan carries an average of 1.3 LeX motifs, meaning that on average 2.6 LeX units are present on the omega-1 glycoprotein. To estimate the occurrence of core fucosylation, the data from the α-fucosidase treatment of site N176 were used. As evident from the mass spectra in Figure 4B and 4C, recorded after the removal of antenna fucoses, the vast majority of N176 glycans carry one or two core fucoses. This conclusion was verified by MALDI-TOF/TOF-MS for the high abundant glycans (Table 2). We calculated that 60 % of the glycans at N176 carry two fucoses at the core, 30 % carry one core fucose and 10 % have no core fucosylation. For site N71, when focusing on the twelve most abundant glycan structures of site N71 (Table 2), we calculated that 74 % of these glycans carry two core fucoses, 10 % carry one core fucose and 16 % have no core fucosylation. As already reported for the egg and ES glycoprotein mixture [12;15], the observed difucosylated core structures are expected to be comprised of α1-3,α1-6-linked fucoses. It remains unclear whether the fucose at the mono-fucosylated core is α1-3 or α1-6 linked.

To conclude, the analysis of tryptic glycopeptides by MALDI-TOF/TOF-MS and nano-LC-MS/MS, in combination with β-galactosidase and/or α-fucosidase treatment reveal that the majority of N-glycans of omega-1 express two fucoses on the innermost *N*-acetylglucosamine and contain one or two terminal LeX motifs. Less abundant antenna structures include LN and difucosylated LN, non, mono- and difucosylated LDN and (fucosylated) LN and LDN repeats.

Discussion

Omega-1 is a single glycoprotein in *S. mansoni* SEA that harbors the potent Th2-inducing properties characteristic for this complex antigen mixture [6;9]. Glycans from schistosome egg glycoproteins are ligands for multiple CLRs present on immune cells [20;32], and these glycans appear to be involved in immunomodulatory activities attributed to SEA [5;10]. Prompted by these observations and the lack of structural information about omega-1 glycans, we performed a site-specific analysis of the glycosylation pattern of omega-1.

This study reveals that omega-1 has two fully occupied N-glycosylation sites. Both sites display similar glycan heterogeneity, but with different relative abundances of the individual glycans present (Figure 2 and Table 2). All glycans on omega-1 are of a diantennary complex type, and most display an α3 and/or α6 fucosylation of the innermost *N*-acetylglucosamine (Tables 1 and 2). LeX was found to be the major antenna motif, but also other terminal glycan elements were found to be expressed on omega-1, including LDN-F, tandem repeats of LeX, and difucosylated LN and LDN. In addition, we searched the LC-MS-derived data for O-glycosylated peptides, focusing on O-glycosylation marker oxonium ions at *m/z* 204 (HexNAc antenna), *m/z* 350 (fucosylated HexNAc antenna), *m/z* 407 (LDN antenna), *m/z* 496 (difucosylated HexNAc

antenna), *m/z* 512 (LeX antenna) and *m/z* 699 (difucosylated LDN antenna). Using these marker ions, we could not find any indications for O-linked glycosylation on omega-1.

The occurrence of these types of N-glycan elements in a schistosome egg glycoprotein is in line with data generated by non-protein-specific analysis of the N-glycans of *S. mansoni* egg glycoproteins in SEA [12] as well as in ES [15], the latter being a mixture of excretory/secretory glycoproteins of which omega-1 is a major component [16;17]. Simultaneous expression of LDN- and LN-based antenna elements has been reported in the egg glycoprotein mixtures as well as in the protein-specific glycosylation analysis of IPSE/α1 [24]. Based on the LN and LDN backbones,

Table 2. Schematic representation of the most abundant N-glycans detected on omega-1

Glycans[a]	relative abundance on site N176 (%)[b]	relative abundance on site N71 (%)[b]	relative abundance on Omega-1 (%)
	14	14	14
	7	10	9
	8	8	8
	8	4	6
	5	5	5
	4	2	3
	1	5	3
	4	2	3
	4	1	2.5
	2	3	2.5
	2	3	2.5
	2	3	2.5

a Triangle, fucose; light circle, galactose; light square, *N*-acetylgalactosamine; dark square, *N*-acetylglucosamine; dark circle, mannose.

b Numbers are based on glycopeptide signal intensities in MALDI-TOF-MS (site N176) or LC-MS (site N71), in combination with signal intensities from fragmentation and enzyme data for isomeric structures.

both LeX and LDN-F antigens are present on omega-1, most likely due to action of a LeX-type fucosyltransferase (FucT) in *S. mansoni* eggs that is also capable of transferring fucose to the GlcNAc residue in LDN in addition to that in LN [33]. We also detected difucosylated LN and LDN variants on omega-1. The F-LDN-F element has been previously described in schistosome glycoproteins and glycolipids [12;15;26]. In contrast, the difucosylated LN element has not been detected before in schistosome eggs or ES. This element likely represents the pseudo-LeY motif (Fucα1-3Galβ1-4(Fucα1-3)GlcNAc) as has previously been described in a major fraction of *S. mansoni* cercarial glycolipids [34]. Hypothetically, a difucosylated LN motif also may contain the Fucα1-2Fucα1-3 sequence. This disaccharide sequence is abundantly present on schistosome egg O-glycans [15], glycolipids [26] and free excretory oligosaccharides [35], but only in the context of chito-oligomeric or LDN backbones. We did not find indications for the occurrence of the Fucα1-2Fuc element on omega-1. With respect to the biosynthesis of the different fucosylated elements present in omega-1, some may be formed by the action of the same FucT (e.g. LeX and LDN-F [33]), as has also been suggested for the formation of the Fucα1-3GalNAc linkage in F-LDN-F and the Fucα1-3Gal in pseudo-LeY [34;36]. Still, at least 4 different FucTs appear to be active at the site of production of omega-1, and taking into account the occurrence of the other fucosylated motifs in *S. mansoni* eggs and other life stages, it is not surprising that at least 20 FucT genes are present in the *S. mansoni* genome [37], some of which display highly regulated expression levels by transcriptome analysis [38]. It is unclear at present what the precise acceptor and linkage specificities of these FucTs are, as current annotation based on sequence homology is not sufficient to classify these FucTs.

With respect to the overall set of N-glycans found on ES glycoproteins [15], truncated and high-mannose type glycans as well as core xylosylation observed in a minor set of ES glycoproteins were not found for omega-1. On the other hand, the glycosylation of IPSE/α1, the only other *S. mansoni* egg glycoprotein of which specific glycosylation data is available to date, appears to be highly homologous to omega-1 [24]. IPSE/α1 is produced in the sub-shell area of the schistosome egg, at the same location as omega-1, which suggests that these two proteins, both major constituents of *S. mansoni* ES, are subjected to the same glycosylation machinery. According to Mathieson et al., at least four other major glycoproteins are present in *S. mansoni* egg ES, including thioredoxin and three micro-exon-gene (MEG) proteins [18], and it would be interesting to see if these proteins carry the O-glycans as well as the subset of N-glycans found in ES, but not present on omega-1 and IPSE/α1. In this respect, it must be noted that proteomic analysis of ES by another group led to the identification of 188 proteins [16] instead of only a few [18]. This discrepancy may be explained by the different methods used for the preparation of ES. Furthermore, while Cass et al. analyzed the whole ES mixture [16], Mathieson and Wilson

separated ES proteins on a 2-DE gel and merely investigated the spots visible after Sypro Ruby staining, possibly missing low-abundant proteins [18]. However, in spite of the large differences between the protein contents of ES fractions, in both cases omega-1 and IPSE/α1 were identified as the most abundant ES proteins, underlining also the relative abundance of the glycans they carry in the overall ES glycome.

The finding that omega-1 contains the LeX motif is of importance. In the context of a LNFPIII conjugate, LeX has previously been shown to induce Th2 responses in a mouse model following intranasal immunization [10]. Furthermore, it can stimulate murine DCs *in vitro* towards a type 2 DC capable of inducing the development of Th2 cells from naive mouse-derived CD4+ T cells [11]. Based on these data, it would be tempting to attribute the recently reported Th2-polarizing properties of omega-1 to its LeX structures [6;9]. However, IPSE/α1, which carries virtually identical LeX-containing glycans to omega-1, is not able to induce the strong DC-mediated type 2 responses observed for omega-1 in the same assay [6;24], indicating that in this case also properties provided by the underlying protein backbone play a role. Interestingly, Steinfelder et al. recently demonstrated in an *in vitro* bystander polarization assay that upon treatment with diethyl pyrocarbonate, a chemical which irreversibly modifies histidine residues, omega-1 is no longer able to condition DCs for Th2-induction [9]. Clearly, the possible contributions of the glycan and protein parts to the immunological properties of omega-1 need to be further investigated. In this respect, it is interesting to note that fucosylated glycan structures abundantly present on omega-1, are recognized by CLRs such as DC-SIGN and MR [19;39], which have been reported to mediate internalization of SEA constituents by DCs [20].

The detailed examination of the site-specific glycosylation of omega-1 was made possible by an approach based on MALDI-TOF(/TOF)-MS and nano-LC-MS/(MS) analysis. Importantly, by combining the MS analyses with specific exo-glycosidase treatments, we could validate structural assignments of important glycan elements, exclude potential false interpretations of the MS/MS spectra due to frequently occurring fucose rearrangements [30], and thus provide a solid basis for the identification and characterization of the glycan structures. This methodology, based on gel-derived tryptic glycopeptides, is also easily applicable to many other glycoproteins as it does not require extensive or complicated sample workup.

Materials and Methods

Purification of omega-1

Omega-1 was purified from SEA as previously described [7,23,25]. In short, SEA was prepared from *Schistosoma mansoni* eggs and fractionated by cation exchange chromatography. Omega-1,

together with IPSE/α1 a constituent of the highly cationic egg fraction CEF6, was separated from IPSE/α1 by affinity chromatography using specific anti-IPSE/α1 monoclonal antibodies coupled to an NHS-HiTrap Sepharose column according to the manufacturer's instructions (GE Healthcare, Little Chalfont, UK).

α -Fucosidase treatment for Western blot analysis

Antigens were dissolved in 10 µl 100 mM sodium phosphate buffer, pH 5.0 and treated with α-1-(3,4)-fucosidase from *Xanthomonas manihotis* (0.5 mU; Sigma, Zwijndrecht, The Netherlands) overnight at 37 °C.

To confirm removal of fucoses, omega-1 was reduced by incubation with 0.025 volumes of 200 mM dithiothreitol for 30 minutes at 60°C, after which the antigen solution was mixed with 0.075 volumes of 200 mM iodoacetamide and incubated for 30 minutes in the dark at room temperature. Trypsin (Promega, Leiden, The Netherlands) was added to the sample at a 1:100 trypsin/antigen ratio and incubated overnight at 37°C. After incubation, the digestion was quenched with 1 µl of 5% trifluoroacetic acid. Tryptic digests were measured using MALDI-TOF-mass analysis in the positive ion reflectron mode (results not shown).

Western blot analysis

1 µg of untreated and fucosidase-treated omega-1 was subjected to SDS-PAGE under reducing conditions on a 12% gel using the Mini-Protean Cell system (Bio-rad, Veenendaal, The Netherlands). The proteins were transferred onto a nitrocellulose membrane in a Bio-rad Criterion Blotter system according to manufacturer's instructions. The protein blots were stained as described previously [26]. In short, blots were blocked with BSA and incubated with the primary anti-carbohydrate mAb 128-4F9-A, which binds to LeX antennae. Blots were subsequently incubated with AP-labeled goat-anti-mouse IgG (Caltag; Invitrogen, Breda, The Netherlands) and stained with NBT/BCIP.

Sample preparation for mass spectrometric analysis

10 µg of omega-1 were separated on a 12% polyacrylamide gel by SDS-PAGE electrophoresis under reducing conditions using the Mini-Protean Cell system (Bio-rad) and stained with Colloidal blue (Invitrogen, Groningen, The Netherlands) according to manufacturer's recommendations. The stained omega-1 band (31 kD) was excised and stored in 1% acetic acid at 4°C. The gel piece containing omega-1 was reduced, alkylated and digested with 0.015 µg

trypsin (Promega), as previously described [27]. After digestion, peptides were extracted twice with 20 µl of 0.1% TFA. Extracts were pooled and stored at -20 °C.

Exo-glycosidase treatment for mass spectrometric analysis

Tryptic glycopeptides were treated with β-galactosidase from bovine testis (1 mU; Sigma, Zwijndrecht, the Netherlands) in 10 µl 100 mM sodium phosphate buffer, pH 5.0, for 24 hours at 37°C. α-Fucosidase treatment was performed on tryptic glycopeptides with α1-(3,4)-Fucosidase from *Xanthomonas manihotis* (0.5 mU; Sigma) in 100 mM sodium phosphate buffer, pH 5.0, for 24 hours at 37°C. Part of the α-fucosidase-treated glycopeptides was subsequently treated with β-galactosidase for 24 hours at 37°C.

MALDI-TOF(/TOF) MS

Total tryptic digest of omega-1, as well as glycopeptides after β-galactosidase and/or α-fucosidase treatment, were purified by Zip-Tip µ-C18 following the manufacturer's instructions (Millipore, Billerica, MA, USA), eluted with 10 $mg \cdot ml^{-1}$ DHB in 50% acetonitrile, 0.1% trifluoroacetic acid onto a MALDI target plate and air dried. MALDI-TOF(/TOF)-MS data were obtained using an Ultraflex II time-of-flight mass spectrometer (Bruker-Daltonics, Bremen, Germany) equipped with a LIFT-MS/MS facility. Spectra were acquired in the positive ion reflectron mode. For fragment ion analysis in the tandem time-of-flight (TOF/ TOF) mode, precursors were accelerated to 8 kV and selected in a timed ion gate. Fragment ions generated by metastable decomposition of the precursor in the field-free drift region were further accelerated by 19 kV in the LIFT cell, and their masses were analyzed after the ion reflector passage. MS/MS spectra with fragment ions showing a high mass deviation were subjected to internal calibration using chitobiose cleavage products as calibrant signals.

Nano-HPLC ESI-ion trap-MS(/MS)

Total tryptic digest of omega-1, as well as glycopeptides after β-galactosidase treatment, were applied to a reverse-phase column (PepMap, 3 µm, 75 µm·100 mm; Dionex /LC Packings, Amsterdam, the Netherlands) using an Ultimate 3000 nano-LC system (Dionex /LC Packings). The column was equilibrated at room temperature with eluent A (0.1% formic acid in water) at a flow rate of 200 $nL \cdot min^{-1}$. After injection of the sample, elution conditions were switched to 10% solvent B (95% acetonitrile, 0.1% formic acid), followed by a gradient to 60% B in 45 min and a subsequent isocratic elution of 10 min. The eluate was monitored by absorption at 215 nm.

The LC column was coupled to an Esquire HCT-Ultra ESI-ion trap-MS (Bruker-Daltonics, Bremen, Germany) equipped with an online nanospray source operating in the positive-ion mode. For electrospray (1100–1250 V), electropolished, stainless steel LC/MS emitters (150 µm OD, 30 µm ID) from Proxeon A/S (Odense, Denmark) were used. The solvent was evaporated at 175ºC employing a nitrogen stream of 7 L·min^{-1}. Ions from *m/z* 500 to *m/z* 1800 were registered in the MS mode. When operated in the auto MS/MS mode, registering ions from *m/z* 140 to 2200, each MS scan was followed by the acquisition of MS/MS spectra of up to three of the most abundant ions in the MS spectrum.

Acknowledgements

We thank Isabel Catalina for performing initial experiments and Carolien Koeleman for expert technical assistance. This work was supported by the Dutch Organization for Scientific Research (NWO), Grant No CW ECHO 700.55.013.

References

1. Pearce, E. J.; MacDonald, A. S. The immunobiology of schistosomiasis. *Nat. Rev. Immunol.* **2002,** *2* (7), 499-511.
2. Pearce, E. J. Priming of the immune response by schistosome eggs. *Parasite Immunol.* **2005,** *27* (7-8), 265-270.
3. Vella, A. T.; Pearce, E. J. CD4+ Th2 response induced by *Schistosoma mansoni* eggs develops rapidly, through an early, transient, Th0-like stage. *J. Immunol.* **1992,** *148* (7), 2283-2290.
4. Jankovic, D.; Kullberg, M. C.; Caspar, P.; Sher, A. Parasite-induced Th2 polarization is associated with down-regulated dendritic cell responsiveness to Th1 stimuli and a transient delay in T lymphocyte cycling. *J. Immunol.* **2004,** *173* (4), 2419-2427.
5. Okano, M.; Satoskar, A. R.; Nishizaki, K.; Abe, M.; Harn, D. A., Jr. Induction of Th2 responses and IgE is largely due to carbohydrates functioning as adjuvants on Schistosoma mansoni egg antigens. *J. Immunol.* **1999,** *163* (12), 6712-6717.
6. Everts, B.; Perona-Wright, G.; Smits, H. H.; Hokke, C. H.; Van der Ham, A. J.; Fitzsimmons, C. M.; Doenhoff, M. J.; Van der Bosch, J.; Mohrs, K.; Haas, H.; Mohrs, M.; Yazdanbakhsh, M.; Schramm, G. Omega-1, a glycoprotein secreted by *Schistosoma mansoni* eggs, drives Th2 responses. *J. Exp. Med.* **2009,** *206* (8), 1673-1680.
7. Dunne, D. W.; Lucas, S.; Bickle, Q.; Pearson, S.; Madgwick, L.; Bain, J.; Doenhoff, M. J. Identification and partial purification of an antigen (omega 1) from *Schistosoma mansoni* eggs which is putatively hepatotoxic in T-cell deprived mice. *Trans. R. Soc. Trop. Med. Hyg.* **1981,** *75* (1), 54-71.
8. Fitzsimmons, C. M.; Schramm, G.; Jones, F. M.; Chalmers, I. W.; Hoffmann, K. F.; Grevelding, C. G.; Wuhrer, M.; Hokke, C. H.; Haas, H.; Doenhoff, M. J.; Dunne, D. W. Molecular characterization of omega-1: a hepatotoxic ribonuclease from *Schistosoma mansoni* eggs. *Mol. Biochem. Parasitol.* **2005,** *144* (1), 123-127.
9. Steinfelder, S.; Andersen, J. F.; Cannons, J. L.; Feng, C. G.; Joshi, M.; Dwyer, D.; Caspar, P.; Schwartzberg, P. L.; Sher, A.; Jankovic, D. The major component in schistosome eggs responsible for conditioning dendritic cells for Th2 polarization is a T2 ribonuclease (omega-1). *J. Exp. Med.* **2009,** *206* (8), 1681-1690.
10. Okano, M.; Satoskar, A. R.; Nishizaki, K.; Harn, D. A., Jr. Lacto-N-fucopentaose III found on *Schistosoma mansoni* egg antigens functions as adjuvant for proteins by inducing Th2-type response. *J. Immunol.* **2001,** *167* (1), 442-450.

11. Thomas, P. G.; Carter, M. R.; Atochina, O.; 'Dara, A. A.; Piskorska, D.; McGuire, E.; Harn, D. A. Maturation of dendritic cell 2 phenotype by a helminth glycan uses a Toll-like receptor 4-dependent mechanism. *J. Immunol.* **2003,** *171* (11), 5837-5841.
12. Khoo, K. H.; Chatterjee, D.; Caulfield, J. P.; Morris, H. R.; Dell, A. Structural mapping of the glycans from the egg glycoproteins of *Schistosoma mansoni* and *Schistosoma japonicum*: identification of novel core structures and terminal sequences. *Glycobiology* **1997,** *7* (5), 663-677.
13. Van Remoortere, A.; Hokke, C. H.; Van dam, G. J.; Van Die, I.; Deelder, A. M.; Van den Eijnden, D. H. Various stages of schistosoma express Lewis(x), LacdiNAc, GalNAcbeta1-4 (Fucalpha1-3)GlcNAc and GalNAcbeta1-4(Fucalpha1-2Fucalpha1-3)GlcNAc carbohydrate epitopes: detection with monoclonal antibodies that are characterized by enzymatically synthesized neoglycoproteins. *Glycobiology* **2000,** *10* (6), 601-609.
14. Huang, H. H.; Tsai, P. L.; Khoo, K. H. Selective expression of different fucosylated epitopes on two distinct sets of *Schistosoma mansoni* cercarial O-glycans: identification of a novel core type and Lewis X structure. *Glycobiology* **2001,** *11* (5), 395-406.
15. Jang-Lee, J.; Curwen, R. S.; Ashton, P. D.; Tissot, B.; Mathieson, W.; Panico, M.; Dell, A.; Wilson, R. A.; Haslam, S. M. Glycomics analysis of Schistosoma mansoni egg and cercarial secretions. *Mol. Cell Proteomics.* **2007,** *6* (9), 1485-1499.
16. Cass, C. L.; Johnson, J. R.; Califf, L. L.; Xu, T.; Hernandez, H. J.; Stadecker, M. J.; Yates, J. R., III; Williams, D. L. Proteomic analysis of *Schistosoma mansoni* egg secretions. *Mol. Biochem. Parasitol.* **2007,** *155* (2), 84-93.
17. Ashton, P. D.; Harrop, R.; Shah, B.; Wilson, R. A. The schistosome egg: development and secretions. *Parasitology* **2001,** *122* (Pt 3), 329-338.
18. Mathieson, W.; Wilson, R. A. A comparative proteomic study of the undeveloped and developed *Schistosoma mansoni* egg and its contents: The miracidium, hatch fluid and secretions. *Int. J. Parasitol.* **2010,** *40*, 617–628.
19. Van Liempt, E.; Bank, C. M.; Mehta, P.; Garcia-Vallejo, J. J.; Kawar, Z. S.; Geyer, R.; Alvarez, R. A.; Cummings, R. D.; Van Kooyk, Y.; Van Die, I. Specificity of DC-SIGN for mannose- and fucose-containing glycans. *FEBS Lett.* **2006,** *580* (26), 6123-6131.
20. Van Liempt, E.; Van Vliet, S. J.; Engering, A.; Garcia Vallejo, J. J.; Bank, C. M.; Sanchez-Hernandez, M.; Van Kooyk, Y.; Van Die, I. *Schistosoma mansoni* soluble egg antigens are internalized by human dendritic cells through multiple C-type lectins and suppress TLR-induced dendritic cell activation. *Mol. Immunol.* **2007,** *44* (10), 2605-2615.
21. Shepherd, V. L.; Campbell, E. J.; Senior, R. M.; Stahl, P. D. Characterization of the mannose/fucose receptor on human mononuclear phagocytes. *J. Reticuloendothel. Soc.* **1982,** *32* (6), 423-431.
22. Van Vliet, S. J.; Saeland, E.; Van Kooyk, Y. Sweet preferences of MGL: carbohydrate specificity and function. *Trends Immunol.* **2008,** *29* (2), 83-90.
23. Schramm, G.; Falcone, F. H.; Gronow, A.; Haisch, K.; Mamat, U.; Doenhoff, M. J.; Oliveira, G.; Galle, J.; Dahinden, C. A.; Haas, H. Molecular characterization of an interleukin-4-inducing factor from *Schistosoma mansoni* eggs. *J. Biol. Chem.* **2003,** *278* (20), 18384-18392.
24. Wuhrer, M.; Balog, C. I.; Catalina, M. I.; Jones, F. M.; Schramm, G.; Haas, H.; Doenhoff, M. J.; Dunne, D. W.; Deelder, A. M.; Hokke, C. H. IPSE/alpha-1, a major secretory glycoprotein antigen from schistosome eggs, expresses the Lewis X motif on core-difucosylated N-glycans. *FEBS J.* **2006,** *273* (10), 2276-2292.
25. Dunne, D. W.; Jones, F. M.; Doenhoff, M. J. The purification, characterization, serological activity and hepatotoxic properties of two cationic glycoproteins (alpha 1 and omega 1) from *Schistosoma mansoni* eggs. *Parasitology* **1991,** *103 Pt 2*, 225-236.
26. Robijn, M. L.; Wuhrer, M.; Kornelis, D.; Deelder, A. M.; Geyer, R.; Hokke, C. H. Mapping fucosylated epitopes on glycoproteins and glycolipids of *Schistosoma mansoni* cercariae, adult worms and eggs. *Parasitology* **2005,** *130* (Pt 1), 67-77.
27. Steen, H.; Pandey, A.; Andersen, J. S.; Mann, M. Analysis of tyrosine phosphorylation sites in signaling molecules by a phosphotyrosine-specific immonium ion scanning method. *Sci. STKE.* **2002,** *2002* (154), l16.
28. Van Die, I.; Cummings, R. D. Glycan gimmickry by parasitic helminths: a strategy for modulating the host immune response? *Glycobiology* **2010,** *20* (1), 2-12.
29. Agoston, K.; Kerekgyarto, J.; Hajko, J.; Batta, G.; Lefeber, D. J.; Kamerling, J. P.; Vliegenthart, J. F. Synthesis of fragments of the glycocalyx glycan of the parasite Schistosoma mansoni. *Chemistry.* **2002,** *8* (1), 151-161.

30. Wuhrer, M.; Koeleman, C. A.; Hokke, C. H.; Deelder, A. M. Mass spectrometry of proton adducts of fucosylated N-glycans: fucose transfer between antennae gives rise to misleading fragments. *Rapid Commun. Mass Spectrom.* **2006,** *20* (11), 1747-1754.
31. Faveeuw, C.; Mallevaey, T.; Paschinger, K.; Wilson, I. B.; Fontaine, J.; Mollicone, R.; Oriol, R.; Altmann, F.; Lerouge, P.; Capron, M.; Trottein, F. Schistosome N-glycans containing core alpha 3-fucose and core beta 2-xylose epitopes are strong inducers of Th2 responses in mice. *Eur. J. Immunol.* **2003,** *33* (5), 1271-1281.
32. Van Die, I; Van Vliet, S. J.; Nyame, A. K.; Cummings, R. D.; Bank, C. M.; Appelmelk, B.; Geijtenbeek, T. B.; Van Kooyk Y. The dendritic cell-specific C-type lectin DC-SIGN is a receptor for *Schistosoma mansoni* egg antigens and recognizes the glycan antigen Lewis x. *Glycobiology* **2003,** *13* (6), 471-478.
33. Paschinger, K.; Staudacher, E.; Stemmer, U.; Fabini, G.; Wilson, I. B. Fucosyltransferase substrate specificity and the order of fucosylation in invertebrates. *Glycobiology* **2005,** *15* (5), 463-474.
34. Wuhrer, M.; Dennis, R. D.; Doenhoff, M. J.; Lochnit, G.; Geyer, R. *Schistosoma mansoni* cercarial glycolipids are dominated by Lewis X and pseudo-Lewis Y structures. *Glycobiology* **2000,** *10* (1), 89-101.
35. Robijn, M. L.; Koeleman, C. A.; Hokke, C. H.; Deelder, A. M. *Schistosoma mansoni* eggs excrete specific free oligosaccharides that are detectable in the urine of the human host. *Mol. Biochem. Parasitol.* **2007,** *151* (2), 162-172.
36. Meyer, S.; Van Liempt, E.; Imberty, A.; Van Kooyk, Y.; Geyer, H.; Geyer, R.; Van Die, I. DC-SIGN mediates binding of dendritic cells to authentic pseudo-LewisY glycolipids of *Schistosoma mansoni* cercariae, the first parasite-specific ligand of DC-SIGN. *J. Biol. Chem.* **2005,** *280* (45), 37349-37359.
37. Berriman, M.; Haas, B. J.; LoVerde, P. T.; Wilson, R. A.; Dillon, G. P.; Cerqueira, G. C.; Mashiyama, S. T.; Al-Lazikani, B.; Andrade, L. F.; Ashton, P. D.; Aslett, M. A.; Bartholomeu, D. C.; Blandin, G.; Caffrey, C. R.; Coghlan, A.; Coulson, R.; Day, T. A.; Delcher, A.; DeMarco, R.; Djikeng, A.; Eyre, T.; Gamble, J. A.; Ghedin, E.; Gu, Y.; Hertz-Fowler, C.; Hirai, H.; Hirai, Y.; Houston, R.; Ivens, A.; Johnston, D. A.; Lacerda, D.; Macedo, C. D.; McVeigh, P.; Ning, Z.; Oliveira, G.; Overington, J. P.; Parkhill, J.; Pertea, M.; Pierce, R. J.; Protasio, A. V.; Quail, M. A.; Rajandream, M. A.; Rogers, J.; Sajid, M.; Salzberg, S. L.; Stanke, M.; Tivey, A. R.; White, O.; Williams, D. L.; Wortman, J.; Wu, W.; Zamanian, M.; Zerlotini, A.; Fraser-Liggett, C. M.; Barrell, B. G.; El-Sayed, N. M. The genome of the blood fluke *Schistosoma mansoni*. *Nature* **2009,** *460* (7253), 352-358.
38. Fitzpatrick, J. M.; Peak, E.; Perally, S.; Chalmers, I. W.; Barrett, J.; Yoshino, T. P.; Ivens, A. C.; Hoffmann, K. F. Anti-schistosomal intervention targets identified by lifecycle transcriptomic analyses. *PLoS. Negl. Trop. Dis.* **2009,** *3* (11), e543.
39. Taylor, M. E.; Bezouska, K.; Drickamer, K. Contribution to ligand binding by multiple carbohydrate-recognition domains in the macrophage mannose receptor. *J. Biol. Chem.* **1992,** *267* (3), 1719-1726.

Supplementary figures

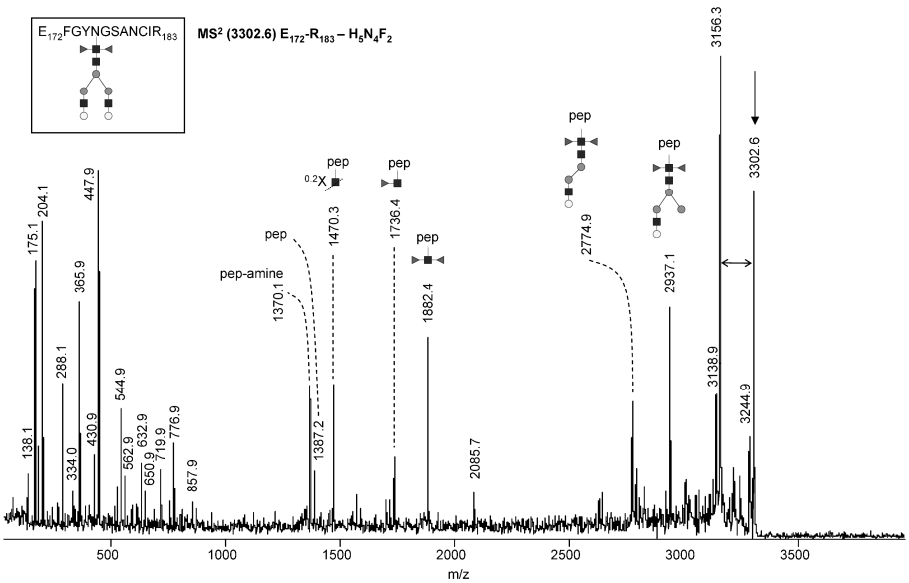

Supplementary figure 1. MS/MS of peptide E172–R183 carrying H5N4F2 N-glycans. The MS/MS spectrum was acquired by MALDI-TOF/TOF-MS of a tryptic digest of omega-1 treated with α-fucosidase. The single-headed arrow indicates the parent ion. Differences in fucose content are indicated by double-headed arrows. Triangle, fucose; light circle, galactose; dark square, *N*-acetylglucosamine; dark circle, mannose.

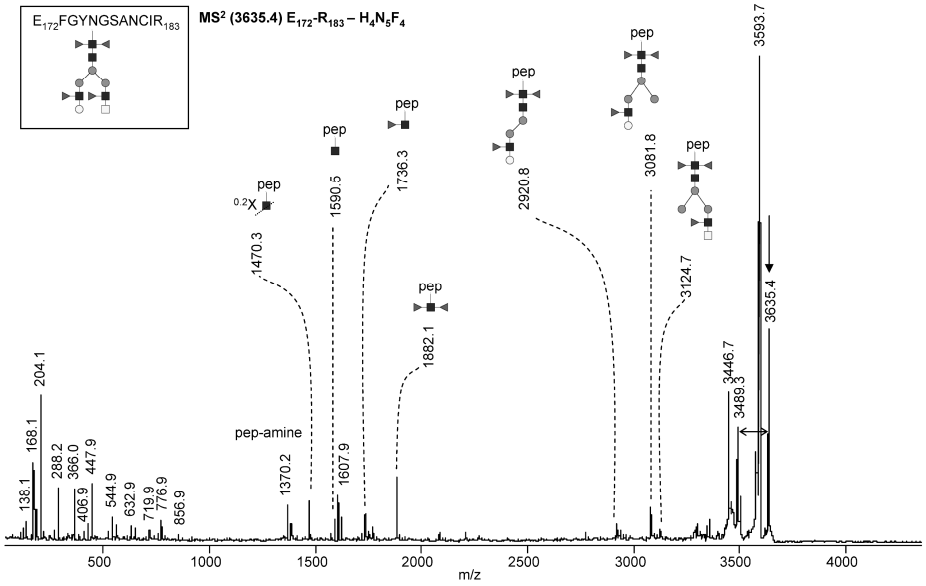

Supplementary figure 2. MS/MS of peptide E172–R183 carrying H4N5F4 N-glycans. The MS/MS spectrum was acquired by MALDI-TOF/TOF-MS of a tryptic digest of omega-1. The single-headed arrow indicates the parent ion. Differences in fucose content are indicated by double-headed arrows. Triangle, fucose; light circle, galactose; dark square, *N*-acetylglucosamine; light square, *N*-acetylgalactosamine; dark circle, mannose.

Supplementary Table 1. Omega-1 glycopeptide species detected after trypsin digestion and α-fucosidase treatment

Glycan composition[a]	Glycopeptide signal (*m/z*)[b]	Relative peak height (%)[c]	Fragment ions[d]	Proposed structures[e]
$H_4N_3F_1$	2791.1 [M+H]$^+$ (β-gal: 2629.5; -1 Hex)	3		1 LN, 1 core fucose
$H_4N_3F_2$	2937.4 [M+H]$^+$ (β-gal: 2775.5; -1 Hex)	7	1736.5 (pep^1+N_1F_1; 0.5) 1882.6 (pep^1+N_1F_2; 1.0) 2572.2 (pep^1+$H_3N_2F_2$) - H_1N_1	1 LN, ^{3,6}F 
$H_5N_3F_1$	2953.4 [M+H]$^+$ (β-gal: 2953.6, -0 Hex)	2		Mono-fucosylated core
H_5N_4	3010.5 [M+H]$^+$ (β-gal: 2686.4; -2 Hex)	10	1590.7 (pep^1+N_1) 2483.2 (pep^1+H_3N_3) - H_2N_1 2645.4 (pep^1+H_4N_3) - H_1N_1	2 LN, no core fucosylation 
H_4N_5	3051.4 [M+H]$^+$ (β-gal: 2889.1; -1 Hex)	2		1 LN, 1 LDN, no core fucosylation 
$H_5N_3F_2$	3099.0 [M+H]$^+$ (β-gal: 3099.1; -0 Hex)	1		1 LN, ^{3,6}F
$H_6N_3F_1$	3115.1 [M+H]$^+$	2		Mono-fucosylated core
$H_4N_4F_2$	3140.1 [M+H]$^+$ (β-gal: 2978.6; -1 Hex)	3		1LN and 1 HexNAc, ^{3,6}F
$H_5N_4F_1$	3156.6 [M+H]$^+$ (β-gal: 2832.5; -2 Hex)	17	1590.6 (pep^1+N_1) 1736.6 (pep^1+N_1F_1) 3629.3 (pep^1+$H_3N_3F_1$) - H_2N_1 2791.4 (pep^1+$H_4N_3F_1$) - H_1N_1	2 LN, mono-core fucosylated 
$H_4N_5F_1$	3197.9 [M+H]$^+$ (β-gal: 3035.7; -1 Hex)	4	1736.7 (pep^1+N_1F_1) 2628.4 (pep^1+$H_3N_3F_1$) - H_1N_2 2790.7 (pep^1+$H_4N_5F_1$) - N_2 2833.4 (pep^1+$H_3N_4F_1$) - H_1N_1	1 LN, 1 LDN, mono-core fucosylated 
$H_4N_4F_3$	3286.2 [M+H]$^+$ (β-gal: 3124.5; -1 Hex)	3		
$H_5N_4F_2$	3302.6 [M+H]$^+$ (β-gal: 2978.6; -2 Hex)	30	1736.4 (pep^1+N_1F_1; 0.4) 1882.4 (pep^1+N_1F_2; 1.0) 2774.9 (pep^1+$H_3N_3F_2$) - H_2N_1 2937.1 (pep^1+$H_4N_3F_2$) - H_1N_1	2 LN, ^{3,6}F 
$H_4N_5F_2$	3343.1 [M+H]$^+$ (β-gal: 3181.7; -1 Hex)	7	1590.8 (pep^1+N_1) 1736.9 (pep^1+N_1F_1; 0.33) 1882.7 (pep^1+N_1F_2; 1.0) 2936.3 (pep^1+$H_4N_3F_2$) - N_2 2979.2 (pep^1+$H_3N_4F_2$) - H_1N_1	1 LN, 1 LDN, ^{3,6}F 
$H_5N_4F_3$	3448.9 [M+H]$^+$ (β-gal: 3125.5; -2 Hex)	3		
$H_4N_5F_3$	3489.7 [M+H]$^+$ (β-gal: 3327.9; - 1 Hex)	1		1LN, 1 fucosylated LDN, ^{3,6}F 
$H_4N_5F_4$	3635.8 [M+H]$^+$ (β-gal: 3473.3; -1 Hex, and 3312.7; -2 Hex)	2		^{3,6}F
$H_6N_5F_2$	3668.1 [M+H]$^+$ (β-gal: 3343.1; -2 Hex)	2		1 LN, 1 di-LN, ^{3,6}F
$H_6N_5F_3$	3813.6 [M+H]$^+$ (β-gal: 3489.6; -2 Hex)	1		^{3,6}F

a Glycan compositions are given in terms of hexose (H), *N*-acetylhexosamine (N) and fucose (F).

b Monoisotopic masses of glycopeptide precursors are given throughout. Glycopeptides are singly positively charged, as registered by MALDI-TOF-MS. For many glycopeptides, masses after β-galactosidase (β-gal) treatment are listed and the loss of n hexose is concluded (- n hex).

c Relative peak height is expressed as a percentage of cumulative peak height.

d Fragment ions were determined by MALDI-TOF/TOF-MS. Pep1 corresponds to peptide E_{172}FGYNGSANCIR$_{183}$ containing glycosylation site N176.

e Proposed glycan structures are deduced from glycopeptide MS after enzyme treatments and fragmentation data. Triangle, fucose; light circle, galactose; light square, *N*-acetylgalactosamine; dark square, *N*-acetylglucosamine; dark circle, mannose.